




Kerr isolated horizon revisited: Caustic-free congruence and adapted tetrad

Aleš Flandera ^{*}, David Kofroň [†] and Tomáš Ledvinka [‡]
*Institute of Theoretical Physics, Faculty of Mathematics and Physics,
Charles University, V Holešovičkách 2, 180 00 Prague, Czech Republic*
(Dated: March 31, 2026)

We revisit the near-horizon description of the Kerr space-time in the isolated horizon formalism using a non-twisting null geodesic congruence and eliminate the coordinate and geodesic pathologies that arise when the Carter constant of motion is globally fixed to a single constant. Adopting instead a previously proposed choice of the Carter constant which depends on the polar angle on the horizon, we obtain an analytic construction of the Newman–Penrose tetrad adapted to isolated horizons together with horizon-adapted coordinates in which its defining properties are manifest. We compute the associated curvature scalars and provide initial data on characteristics for the isolated horizon. In addition to an analytical solution, derived by leveraging extensive results on Kerr null geodesics, we develop two complementary series expansions and outline a practical numerical recipe to make the construction readily usable. Relative to earlier treatments, our formulation avoids caustic-induced breakdowns and incomplete coordinate coverage while yielding a detailed description of the Kerr black hole in the isolated horizon approach.

I. INTRODUCTION

The framework of isolated horizons provides a quasi-local description of black-hole boundaries that is independent of the space-time’s asymptotics, making it ideal for analyzing locally equilibrium settings embedded within fully time-dependent space-times. Within this approach, the geometry of the horizon is encoded in its intrinsic two-metric and its evolution in an equivalence class $[\ell^a]$.

Crucially, this formalism establishes quasi-local notions of mass, angular momentum, and surface gravity based solely on this intrinsic horizon geometry, e.g. [1–3]. Given the physical significance of the Kerr solution, the specific properties of its intrinsic horizon geometry have been thoroughly studied to ensure these quasi-local quantities reproduce standard results, e.g. [3, 4].

In order to describe the space-time in the vicinity of an isolated horizon, Krishnan introduced a Newman–Penrose tetrad together with the conditions it must satisfy to represent an isolated horizon, [5]. However, even when an explicit space-time metric is available, identifying a tetrad that is adapted to the isolated horizon — that is, one that satisfies these conditions — has proven difficult.

Scholtz constructed such a tetrad for the Kerr–Newman family, [6], by applying transformations to the well-known Kinnersley tetrad so that it is both *non-twisting* and *parallel-propagated* along its generators. This marked the first fully consistent isolated horizon description of a rotating, charged black hole. However, the difficulties involved resulted in a tetrad that was given analytically but not explicitly (except on the horizon).

Recently, [7] revisited the construction for the uncharged Kerr space-time. First, the earlier result of [6] is

completed by an explicit expression for the adapted tetrad. More importantly, it was observed that the original choice of the Carter constant and, hence, the null generators from [6], leads either to caustics or coordinates that do not cover the whole space-time (depending on the choice of the other constants of motion). Moreover, an improved choice of the Carter constant has been proposed in [7], which, unlike the one from [6], is not constant. Following an extensive computation, analytical expressions for both the Carter integral of motion and the transversal vector n^a were found in [7] in terms of Weierstrass functions. However, the other tetrad vectors remained unavailable, as did all the Newman–Penrose scalars.

Nevertheless, both [6] and [7] assume prior knowledge of the complete space-time structure: the metric and a Newman–Penrose tetrad are taken as given from the outset. In contrast, [8] demonstrates that the assumption of global spherical symmetry alone is sufficient to yield a particular isolated horizon. A natural continuation of this line of work would be to build on the refined tetrad introduced in [7] and develop an analytic slow-rotation expansion of the Kerr isolated horizon. However, one can instead exploit the construction of parallel-propagated frames based on the hidden symmetries of Kerr space-times, together with recent results on Kerr geodesic congruences, to remove any restriction on the value of the Kerr rotation parameter a . We found the treatment of parallel-propagated frames by Kubizňák et al., [9], and the compendium of null geodesics by Gralla and Lupsasca, [10], useful. Thus, in this paper, we present a construction of the non-twisting null congruence defined by its properties on the horizon that aligns with the geometry of the Kerr black hole space-time in the isolated horizon approach.

Since we build upon two previous papers, we do not repeat the detailed introduction to isolated horizons and Newman–Penrose formalism. Instead, we only briefly describe the Newman–Penrose quantities as they appear in the text, and we refer the reader to [5–7] for further

* flandera.ales@utf.mff.cuni.cz

† d.kofron@gmail.com

‡ tomas.ledvinka@mff.cuni.cz

details.

The paper is structured as follows: In Sec. II, we introduce a *general null geodesic congruence*, establish most of the notation used, and describe the choice of the Carter constant of motion proposed by [7]. Section III constructs the Kerr black hole *tetrad adapted to isolated horizons* in Kerr null coordinates. For most of the construction, we consider a general Carter constant of motion and employ the particular choice only where necessary. We discuss the connection between the adapted tetrad and the Kinnersley tetrad and derive the initial data on characteristics (the horizon and a transversal hypersurface) for the isolated horizon. Section IV presents *coordinates adapted to the isolated horizon* [5] and the corresponding form of the Newman–Penrose tetrad. Moreover, the conditions of an axial isolated horizon, as defined by [11], are discussed. Section V focuses on previously implicitly defined functions, including the *Carter constant* and the *affine parameter* of the geodesics. They are first analyzed analytically, producing complex expressions, and then approximated via two different series expansions: 1) in the radial coordinate around the horizon and 2) in the rotational parameter a . We also provide a recipe for a numerical solution.

To support transparency and reproducibility, the results presented in this work are accompanied by a set of Wolfram Mathematica notebooks that document selected underlying calculations, intermediate steps, and numerical evaluations. These materials are made available to the reader through an openly accessible repository hosted on Zenodo, [12]. The notebooks allow independent verification of the results and provide a practical resource for reproducing and extending the analyses reported in this paper.

II. NON-TWISTING NULL GEODESIC CONGRUENCE

The Kerr metric in null coordinates, that is regular at the horizon, takes the form, [13]:¹

$$\begin{aligned} d\mathfrak{s}^2 = & \left(1 - \frac{2Mr}{\Sigma}\right) dv^2 - 2 dv dr \\ & + \frac{4aMr \sin^2 \theta}{\Sigma} dv d\phi + 2a \sin^2 \theta dr d\phi \\ & - \Sigma d\theta^2 + \frac{\sin^2 \theta}{\Sigma} (\Delta a^2 \sin^2 \theta - \Sigma_0^2) d\phi^2, \end{aligned} \quad (1)$$

¹ In order to make a clear distinction between different coordinates and symbols, we use the following color map of symbols: the (Krishnan) coordinates adapted to the isolated horizon are highlighted in red color, while Kerr null coordinates (and repeating expressions of them) are colored teal. Moreover, the Newman–Penrose quantities, such as the tetrad vectors, derivatives, and scalars, are marked in blue and metric functions green. Finally, olive is used for physical constants.

where

$$\Delta = r^2 - 2Mr + a^2, \quad (2)$$

$$\varrho = r + ia \cos \theta, \quad (3)$$

$$\Sigma = r^2 + a^2 \cos^2 \theta, \quad (4)$$

$$\Sigma_0 = r^2 + a^2. \quad (5)$$

In these coordinates, the general null geodesic congruence n_G^a implied by the Carter equations [14] has components

$$n_G^v = -\frac{a^2 E \sin^2 \theta + aL + \frac{\Sigma_0}{\Delta} (\sqrt{R} - P)}{\Sigma}, \quad (6a)$$

$$n_G^r = \epsilon_r \frac{\sqrt{R}}{\Sigma}, \quad (6b)$$

$$n_G^\theta = \epsilon_\theta \frac{\sqrt{S}}{\Sigma}, \quad (6c)$$

$$n_G^\phi = -\frac{aE + L \sin^{-2} \theta + \frac{a}{\Delta} (\sqrt{R} - P)}{\Sigma}, \quad (6d)$$

where

$$P = aL + E\Sigma_0, \quad (7)$$

$$R = P^2 - K\Delta, \quad (8)$$

$$S = K - (L + aE)^2 + (a^2 E^2 - L^2 \sin^{-2} \theta) \cos^2 \theta, \quad (9)$$

and E is energy, L is angular momentum, and K is the Carter constant of motion. We consider (6) as a space-time vector field rather than one restricted along a particular null geodesic, so these constants of motion must satisfy

$$n_G^a \nabla_a E = 0, \quad n_G^a \nabla_a L = 0, \quad n_G^a \nabla_a K = 0. \quad (10)$$

Since we want n^a to be inward pointing, as per [5], we need to choose the radial square root sign as $\epsilon_r = -1$.

As previously indicated, we consider the *non-twisting* null geodesic congruence proposed by [7], characterized by

$$n_G^a dx^a = du, \quad (11)$$

where the role of u as a null coordinate will be explained in Sec. IV. As argued in [6], to obtain a non-twisting congruence n_G^a that exists everywhere, we have to put $L = 0$. Following the suggestion of [7], we also single out a particular choice of the Carter constant at the horizon that not only corrects the singular behavior at the axis of the congruence chosen in [6], but also leads to vanishing n_G^θ at the horizon.² The geodesic starting at the horizon with $r \doteq r_p$ and $\theta \doteq \theta_p$ (by \doteq we denote equality at the

² Note that, for the Kinnersley tetrad, this component is vanishing everywhere.

horizon and all functions are evaluated on the horizon, e.g. $\Sigma_0 \doteq r_p^2 + a^2$) has

$$K = a^2 \sin^2 \theta_p. \quad (12)$$

Thus, all geodesics in the congruence will have the same E and L , but each one retains the value of K it acquires when it starts at the horizon at $\theta \doteq \theta_p$. Moreover, θ_p will become the coordinate ϑ adapted to the isolated horizon in Sec. IV.

Off the horizon, K is determined by the requirement of geodesic congruence

$$n_G^a \nabla_a K = 0. \quad (13)$$

With the choice $E = 1$ and $L = 0$, we have

$$\sqrt{R} \stackrel{E=1, L=0}{=} \sqrt{\Sigma_0^2 - K \Delta}, \quad (14)$$

$$\sqrt{S} \stackrel{E=1, L=0}{=} \sqrt{K - a^2 \sin^2 \theta}, \quad (15)$$

and condition (13) translates to:

$$-\sqrt{\Sigma_0^2 - K \Delta} K_{,r} + \epsilon_\theta \sqrt{K - a^2 \sin^2 \theta} K_{,\theta} = 0. \quad (16)$$

Obviously, Eq. (16) states that K is constant along any single null ray, but it varies over the manifold. Coordinates r, θ of such a ray starting at the horizon satisfy the implicit equation

$$\int_{\theta_p}^{\theta} \frac{d\theta'}{\epsilon_\theta \sqrt{K - a^2 \sin^2 \theta'}} + \int_{r_p}^r \frac{dr'}{\sqrt{\Sigma_0'^2 - K \Delta'}} = 0. \quad (17)$$

When an explicit dependence of the Carter constant on the horizon coordinate θ_p , such as $K = a^2 \sin^2 \theta_p$, is substituted into this equation, it becomes an implicit equation for $\theta_p(r, \theta)$ and, therefore, also for $K(r, \theta)$. It is straightforward to see that we must set $\epsilon_\theta = \text{sign}(\cos \theta) \text{sign}(r - r_p)$ so that the integrals have opposite signs. Moreover, the Carter constant must satisfy

$$K(r, 0) = K(r, \pi) = 0, \quad K(r, \frac{\pi}{2}) = a^2, \quad (18)$$

we will discuss the behavior at the axis and equator later in Sec. V. We will meet the implicit Eq. (17) expressed in terms of elliptic integrals in Sec. V A.

Because (17) involves elliptic integrals, we cannot write down a closed-form solution for $K(r, \theta)$. Nevertheless, note that implicit equations are nothing exceptional; even simple Newtonian orbital motion requires solving the so-called Kepler (transcendental) equation either numerically or via series expansions. We will discuss both approaches in Sec. V.

To simplify the following expressions, we define

$$\mathbb{K}_r \equiv \sqrt{\Sigma_0^2 - K \Delta}, \quad (19)$$

$$\mathbb{K}_\theta \equiv \epsilon_\theta \sqrt{K - a^2 \sin^2 \theta}. \quad (20)$$

Note that, thanks to the inclusion of ϵ_θ in \mathbb{K}_θ , the function has continuous spatial derivatives at $r = r_p$ and $\theta = \pi/2$.

Apart from the vanishing twist, the expansion of the congruence of n^a is also worth mentioning. It is given by:

$$\hat{\Theta}_n = \frac{1}{\Sigma} \left(\mathbb{K}_\theta \cot \theta + \mathbb{K}_{\theta,\theta} - \mathbb{K}_{r,r} \right). \quad (21)$$

Note that in the Newman–Penrose formalism, we have $\hat{\Theta}_n \equiv 2 \text{Re } \mu$. The expansion must be finite. The term \mathbb{K}_r is real and finite for $r \in (0, \infty)$, and so is its derivative. On the other hand, the regularity of the term $\mathbb{K}_\theta \cot \theta$ on the axis requires \mathbb{K}_θ to be $\mathcal{O}(\sin \theta)$ (as $\theta \rightarrow 0$ and $\theta \rightarrow \pi$). Oftentimes, it is also required that the expansion is negative, e.g. for smooth transitions from a dynamical horizon (with this property) to an isolated one (which does not require the property). This imposes further limitations on the choice of K . See [15] for discussion. Notice that our choice of K does satisfy all these conditions.

To conclude our discussion of the null geodesic congruence, we illustrate the behavior of the transversal geodesic congruences in Fig. 1, which is plotted in the Kerr–Schild Cartesian coordinates; a reference for these coordinates and the corresponding transformation relations can be found in [13, Sec. 5.3.7]. It can be seen that the improved choice (12) ensures that there are no caustics at the axis, while for the simpler choice $K = a^2$ there are caustics at the axis of rotation.

III. THE NON-TWISTING TETRAD

The quantities that describe an isolated horizon are related to a certain Newman–Penrose tetrad that has been described in detail in [5]. Apart from satisfying the usual Newman–Penrose contraction

$$\ell^a n_a = 1, \quad m^a \bar{m}_a = -1, \quad (22)$$

(with all other = 0), the tetrad must have multiple other properties, see any of [5–7] for a review. Unsurprisingly for a (quasi-)local description of a horizon, most of them are prescribed at the horizon itself. For this reason, we start by finding the tetrad on the horizon and extend it off the horizon later.

Although we will use the already thoroughly discussed vector n_G^a and search for the vectors completing it to the Newman–Penrose frame by employing the geometrical properties of the final tetrad, it is practical to also have an existing Newman–Penrose frame as a reference. In many situations, it is convenient to use the Kinnersley tetrad,³ the Newman–Penrose tetrad adapted to the principal null directions, [16], which, in the null coordinates, reads

³ Denoted by (upper or lower) index K.

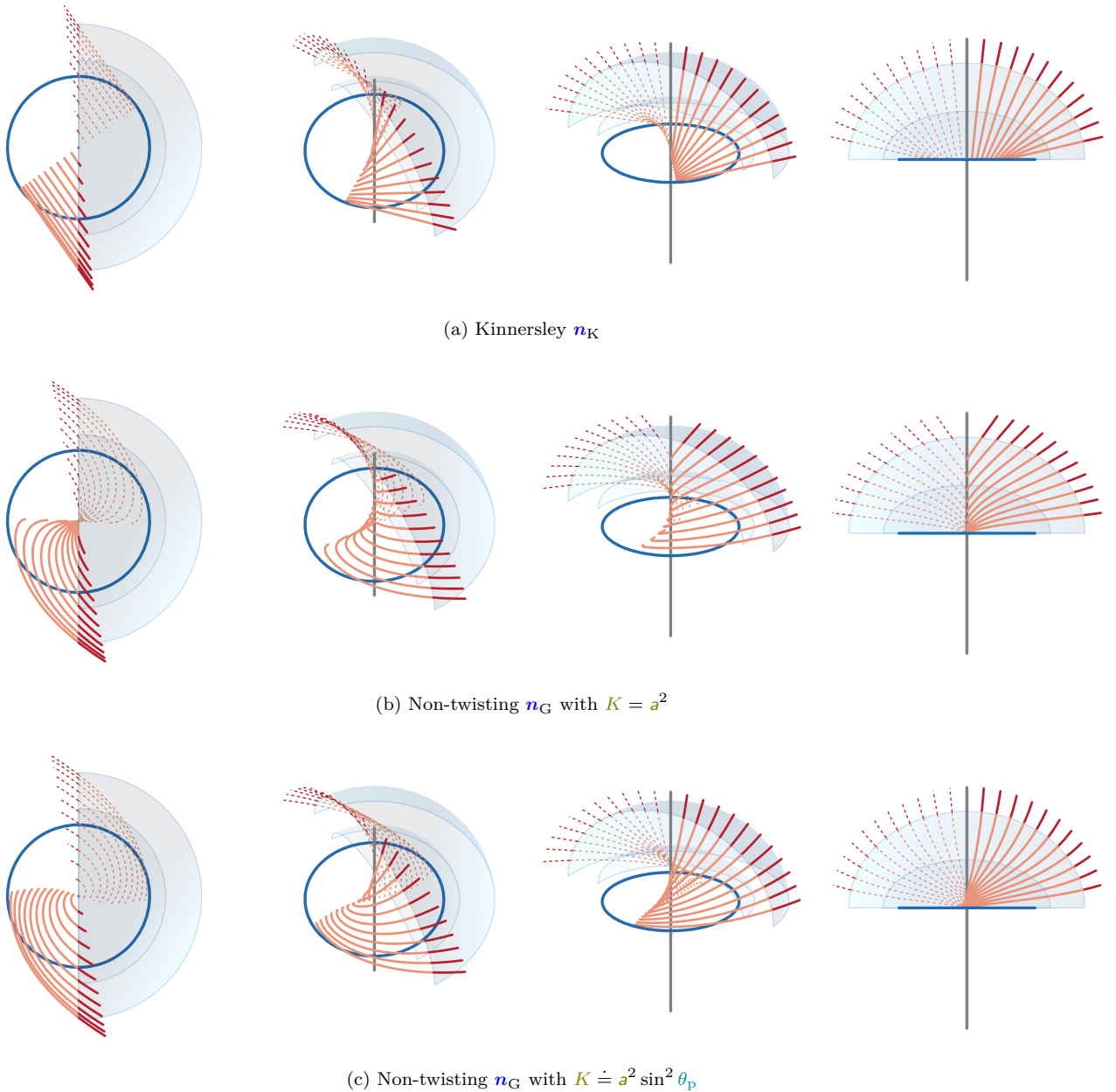


Figure 1. Transversal null geodesics n^a of a Kerr black hole, with parameters $r_p = 2$ and $r_m = 1$, are shown (using a fictitious flat-space projection) in Kerr–Schild Cartesian coordinates for the Kinnersley tetrad and two non-twisting congruences. The grey line marks the rotation axis, the blue circle indicates the ring singularity, and the light blue surfaces represent illustrative portions of the inner and outer horizons. The geodesics are plotted in red, with lighter shading beneath the outer horizon and darker shading above it. Dashed geodesics represent nothing more than geodesics for different azimuthal angle. In the first row (a), the twisting geodesic congruence (unsuitable for isolated horizons) is shown. In the second row (b), the Carter constant is set to $K = a^2$, producing caustics along the axis. In the third row (c), the improved choice $K = a^2 \sin^2 \theta_p$ removes these axis caustics and yields geodesics that pass through the disc to the other sheet, apart from the obstruction at the ring singularity. For each row, the leftmost image gives a view along the axis, the rightmost image shows a perpendicular side view, and the central panels provide intermediate viewpoints along the camera path connecting the two. Supplementary videos providing three-dimensional perspectives of the figures are available through an openly accessible repository hosted on Zenodo, [12].

$$\ell_K = \partial_\nu + \frac{\Delta}{2\Sigma_0} \partial_r + \frac{a}{\Sigma_0} \partial_\phi, \quad (23a)$$

$$n_K = -\frac{\Sigma_0}{\Sigma} \partial_r, \quad (23b)$$

$$m_K = \frac{1}{\sqrt{2}\rho} \left(ia \sin \theta \partial_\nu + \partial_\theta + \frac{i}{\sin \theta} \partial_\phi \right). \quad (23c)$$

This tetrad has a non-zero twist in the direction of n^a and is not suitable for describing isolated horizons by itself. We will show how this can be remedied by means of Lorentz transformations, see Appendix A, which keep the scalar products intact while changing other properties of the frame.

A. The horizon

Let us first discuss a simpler situation. We consider only the restriction of the tetrad fields on the horizon, where we can align the vector n_K^a of the Kinnersley tetrad (23) with the non-twisting null geodesic congruence on the horizon using the following Lorentz transformations:

1. a boost with parameter $A_{K \rightarrow \circ}$ (that changes the Kinnersley tetrad into an intermediate tetrad denoted by the symbol \circ),
2. a rotation about the new ℓ_\circ^a with parameter $c_{\circ \rightarrow \infty}$ (so we end up with a tetrad denoted by ∞).

The parameters are

$$A_{K \rightarrow \circ}^2 = 1, \quad (24)$$

$$c_{\circ \rightarrow \infty} = \frac{ia \sin \theta + \mathbb{K}_\theta}{\sqrt{2}(r_p - ia \cos \theta)}. \quad (25)$$

Notice that the rotation about ℓ^a depends on the choice of the Carter constant of motion K (through \mathbb{K}_θ). All the tetrads stemming from the different choices of this constant are connected by these rotations.

On the horizon, the ∞ -tetrad is identical to the one adapted to isolated horizons (in the Kerr null coordinates). Later, we will see tetrads \bullet and $\bullet\bullet$, corresponding to \circ and ∞ , which will be set also outside (and inside) the horizon, and we will also express the tetrad in the Krishnan coordinates adapted to isolated horizons.

Hence, we are looking for a tetrad that, on the horizon, has the form

$$\ell \doteq \partial_\nu + \frac{a}{\Sigma_0} \partial_\phi, \quad (26a)$$

$$n \doteq \frac{K - 2a^2 \sin^2 \theta}{2\Sigma} \partial_\nu - \frac{\Sigma_0}{\Sigma} \partial_r + \frac{\mathbb{K}_\theta}{\Sigma} \partial_\theta + \frac{a(K - 2\Sigma_0)}{2\Sigma\Sigma_0} \partial_\phi, \quad (26b)$$

$$m \doteq \frac{\mathbb{K}_\theta}{\sqrt{2}\rho} \partial_\nu + \frac{1}{\sqrt{2}\rho} \partial_\theta + \frac{i\Sigma \csc \theta + a\mathbb{K}_\theta}{\sqrt{2}\rho\Sigma_0} \partial_\phi. \quad (26c)$$

Thus, the choice $K = a^2 \sin^2 \theta_p$ proposed by [7] not only ensures that $n^\theta \doteq 0$, but also $m^\nu \doteq 0$.

B. Leaving the horizon

One of the key characteristics of the isolated horizon describing the Krishnan tetrad is that the congruence n^a is accompanied by additional vector fields ℓ^a and m^a that are parallel transported along n^a . We have already employed one miraculous feature of the Kerr geometry that provided the additional integral of motion K . However, there are deeper reasons behind its existence, usually referred to as hidden symmetries of the Kerr metric [9]. In particular, there exists the so-called Killing–Yano anti-symmetric tensor f_{ab} , developed in [17], that not only provides the Carter constant $K = f_{ab} f^b{}_c n^c n^b$, but also allows for the construction of additional parallel transported vector fields.

Using the Kinnersley tetrad (23), the tensor is given as, [18],

$$f_{ab} = -2ir m_{[a}^K \bar{m}_{b]}^K + 2a \cos \theta \ell_{[a}^K n_{b]}^K, \quad (27)$$

where the brackets denote the anti-symmetrization. Its dual $h^{ab} = \frac{1}{2} \varepsilon^{abcd} f_{cd}$ is similarly

$$h_{ab} = 2r \ell_{[a}^K n_{b]}^K + 2ia \cos \theta m_{[a}^K \bar{m}_{b]}^K. \quad (28)$$

Provided that h_{ab} is the principal conformal Killing–Yano tensor, the primary Killing vector k^a is given by

$$k^a = \frac{1}{3} \nabla_b h^{ba}. \quad (29)$$

When searching for the parallel-propagated vectors, we could, in principle, use the same construction as in [7, Sec. IV.]. Namely, to produce the following vectors⁴

$$m_{\text{NPP}}^a = \frac{1}{\sqrt{2K}} (f^a{}_b n^b + i h^a{}_b n^b), \quad (30a)$$

$$\ell_{\text{NPP}}^a = \frac{1}{K} \left(f^a{}_b f^b{}_c n^c + \frac{1}{4} f_{bc} f^{bc} n^a \right), \quad (30b)$$

which are not parallel propagated, and then perform such a rotation about n^a to acquire parallel propagation. Nevertheless, finding the parameter of the rotation for K , which is not constant (in the space-time), involves solving a complicated differential equation.

For this reason, we instead follow the procedure of [9], which is based on earlier works [19–21] and generalizes

⁴ While the tetrad is NP — Newman–Penrose, alas, it is NPP — Not Parallel Propagated.

them, and which directly leads to the following parallel-propagated vector fields:

$$m_{\text{PP}}^a = -\frac{1}{\sqrt{2K}} \left[i (h^a_b + s g^a_b) + f^a_b \right] n^b, \quad (31a)$$

$$\ell_{\text{PP}}^a = \frac{1}{2K} \left[(h^a_b + s g^a_b)(h^b_c + s g^b_c) + f^a_b f^b_c \right] n^c, \quad (31b)$$

where the term in parentheses can be understood as the parallel propagator operator. The scalar field s is required to satisfy, see [9],⁵

$$n^a \nabla_a s = -n_a k^a, \quad (32)$$

so that

$$n^c \nabla_c (h^a_b n^b + s n^a) = 0. \quad (33)$$

In comparison to [9], we have chosen the opposite sign on the right-hand side of (32) (and used the anti-symmetry of the Killing–Yano tensor to factor out the minus in (33)). The reason is as follows. For the Kerr space-time, $k^a = \partial_v$, and condition (32) becomes

$$n^a \nabla_a s = -E \stackrel{E=1}{=} -1. \quad (34)$$

Hence, s is (minus) the affine parameter of the geodesic along n^a . The minus sign has been introduced because, while the vector n^a is inward pointing, it is desirable for

the parameter s to grow outward as a radial coordinate. Thanks to this, we can identify s with the Krishnan radial coordinate; see its definition in [5].

It is worth comparing vectors (31) to (30). Using the following identity

$$f_{ab} f^b_c = h_{ab} h^b_c + \frac{1}{2} h^{de} h_{de}, \quad (35)$$

we can see that (31) is corrected by terms depending on the affine parameter s . Moreover, we include a minus sign in the vector m^a so that its sign convention matches that of the Kinnersley tetrad (and is consistent with the (26) on the horizon).

Before evaluating vectors (31), let us rewrite vector n^a given by (6) for our choice of constants of motion:

$$n = \frac{1}{\Sigma} \left[\left(\frac{\Sigma_0 K}{\mathbb{K}_r + \Sigma_0} - a^2 \sin^2 \theta \right) \partial_v - \mathbb{K}_r \partial_r + \mathbb{K}_\theta \partial_\theta + \left(\frac{aK}{\mathbb{K}_r + \Sigma_0} - a \right) \partial_\phi \right], \quad (36)$$

where we applied

$$\frac{\mathbb{K}_r - \Sigma_0}{\Delta} = -\frac{K}{\mathbb{K}_r + \Sigma_0}, \quad (37)$$

to make the expression explicitly regular on the horizon. The parallel-propagated vectors given by (31) read

$$\begin{aligned} \ell_{\text{PP}} = \frac{1}{2K\Sigma} & \left[\left(\frac{\Sigma_0 K (s + \varrho)(s + \bar{\varrho})}{\mathbb{K}_r + \Sigma_0} + a^2 \sin^2 \theta (\Sigma - s^2 + 2s \mathbb{K}_\theta \cot \theta) \right) \partial_v - \left(\mathbb{K}_r (\Sigma + s^2) - 2rs \Sigma_0 \right) \partial_r \right. \\ & \left. - \left(\mathbb{K}_\theta (\Sigma - s^2) - a^2 s \sin 2\theta \right) \partial_\theta + a \left(\frac{K (s + \varrho)(s + \bar{\varrho})}{\mathbb{K}_r + \Sigma_0} + \Sigma - s^2 + 2s \mathbb{K}_\theta \cot \theta \right) \partial_\phi \right], \end{aligned} \quad (38a)$$

$$\begin{aligned} m_{\text{PP}} = -\frac{i}{\sqrt{2K}\Sigma} & \left[\left(\frac{\Sigma_0 K (s + \bar{\varrho})}{\mathbb{K}_r + \Sigma_0} - a^2 s \sin^2 \theta + i a \bar{\varrho} \mathbb{K}_\theta \sin \theta \right) \partial_v - (s \mathbb{K}_r - \bar{\varrho} \Sigma_0) \partial_r \right. \\ & \left. + (s \mathbb{K}_\theta + i a \bar{\varrho} \sin \theta) \partial_\theta + \left(\frac{aK (s + \bar{\varrho})}{\mathbb{K}_r + \Sigma_0} - as + \frac{i \bar{\varrho} \mathbb{K}_\theta}{\sin \theta} \right) \partial_\phi \right]. \end{aligned} \quad (38b)$$

Notice that the tetrad (38) has no well-defined limit as $a \rightarrow 0$. This is expected since the approach of [9], which we used to construct the frame, requires a non-degenerate principal conformal Killing–Yano tensor — a condition not satisfied by the Schwarzschild metric. This behavior

will be corrected at the end of this section in Eq. (48) by a constant Lorentz transformation. Nevertheless, we postpone this trivial operation and first discuss the properties of this intermediate tetrad with a more compact form. Using the Kinnersley tetrad, the parallel-propagated one can be neatly expressed as

⁵ We deliberately choose the opposite sign on the right-hand side, in

comparison to [9]; the rationale for this will become clear below.

$$\begin{pmatrix} \ell_{\text{PP}} \\ n_{\text{PP}} \\ m_{\text{PP}} \\ \bar{m}_{\text{PP}} \end{pmatrix} = \begin{pmatrix} \frac{(s+\varrho)(s+\bar{\varrho})}{2K} & \frac{(s-\varrho)(s-\bar{\varrho})}{2K} & \frac{(s-\varrho)(s+\bar{\varrho})}{2K} & \frac{(s+\varrho)(s-\bar{\varrho})}{2K} \\ 1 & 1 & 1 & 1 \\ -i\frac{s+\bar{\varrho}}{\sqrt{2K}} & -i\frac{s-\bar{\varrho}}{\sqrt{2K}} & -i\frac{s+\bar{\varrho}}{\sqrt{2K}} & -i\frac{s-\bar{\varrho}}{\sqrt{2K}} \\ i\frac{s+\varrho}{\sqrt{2K}} & i\frac{s-\varrho}{\sqrt{2K}} & i\frac{s-\varrho}{\sqrt{2K}} & i\frac{s+\varrho}{\sqrt{2K}} \end{pmatrix} \cdot \begin{pmatrix} \frac{K\Sigma_0}{(\mathbb{K}_r + \Sigma_0)\Sigma} \ell_{\text{K}} \\ \frac{\mathbb{K}_r + \Sigma_0}{2\Sigma_0} n_{\text{K}} \\ \frac{\mathbb{K}_\theta + ia\sin\theta}{\sqrt{2}\bar{\varrho}} m_{\text{K}} \\ \frac{\mathbb{K}_\theta - ia\sin\theta}{\sqrt{2}\varrho} \bar{m}_{\text{K}} \end{pmatrix} \quad (39)$$

The relation of the PP tetrad to the Kinnersley tetrad can be written as a composition of four elementary Lorentz transformations:

1. a boost with parameter $A_{\text{K}\rightarrow\bullet}$,
2. a rotation about the new ℓ_{\bullet}^a with parameter $c_{\bullet\rightarrow\bullet\bullet}$,
3. a rotation about the newest $n_{\bullet\bullet}^a$ with parameter $d_{\bullet\bullet\rightarrow\bullet\bullet\bullet}$,
4. a spin with parameter $\chi_{\bullet\bullet\bullet\rightarrow\text{PP}}$.

Note that these transformations do not commute, and their order is not fixed. The order we suggest is based on the fact that we first set the size of the vectors ℓ^a and n^a , then the direction of n^a which is set by the condition that it is non-twisting. The direction of vector ℓ^a is then fixed, and the spin, which is the only one with some freedom (we will discuss that in Sec. IV A), is performed last. Additional comments on the transformations are made in Sec. D. For the presented order of transformations, the parameters, as determined from the algebraic relation (39), are

$$A_{\text{K}\rightarrow\bullet}^2 = \frac{2\Sigma_0}{\mathbb{K}_r + \Sigma_0}, \quad (40)$$

$$c_{\bullet\rightarrow\bullet\bullet} = \frac{\mathbb{K}_\theta + ia\sin\theta}{\sqrt{2}\bar{\varrho}}, \quad (41)$$

$$d_{\bullet\bullet\rightarrow\bullet\bullet\bullet} = \frac{s-\bar{\varrho}}{\sqrt{2}(\mathbb{K}_\theta + ia\sin\theta)}, \quad (42)$$

$$e^{2i\chi_{\bullet\bullet\bullet\rightarrow\text{PP}}} = -i\frac{\mathbb{K}_\theta - ia\sin\theta}{\sqrt{K}}. \quad (43)$$

It is simple to verify that $A_{\text{K}\rightarrow\circ}$ and $A_{\text{K}\rightarrow\bullet}$ as well as $c_{\circ\rightarrow\circ\circ}$ and $c_{\bullet\rightarrow\bullet\bullet}$ correspond to each other on the horizon, recall Eqs. (24) and (25) respectively. On the horizon, the parameter $\chi_{\bullet\bullet\bullet\rightarrow\text{PP}}$ vanishes for the choice $K \doteq a^2 \sin^2 \theta$.

The Newman–Penrose projections of the Weyl tensor

onto the parallel-propagated tetrad (38) are given by

$$\Psi_0^{\text{PP}} = -\frac{1}{2K} \frac{3\Psi_2^{\text{K}}}{2\bar{\varrho}^2} (s^2 - \bar{\varrho}^2)^2, \quad (44a)$$

$$\Psi_1^{\text{PP}} = -\frac{i}{\sqrt{2K}} \frac{3\Psi_2^{\text{K}}}{2\bar{\varrho}^2} (s^2 - \bar{\varrho}^2) s, \quad (44b)$$

$$\Psi_2^{\text{PP}} = \frac{\Psi_2^{\text{K}}}{2\bar{\varrho}^2} (3s^2 - \bar{\varrho}^2), \quad (44c)$$

$$\Psi_3^{\text{PP}} = i\sqrt{2K} \frac{3\Psi_2^{\text{K}}}{2\bar{\varrho}^2} s, \quad (44d)$$

$$\Psi_4^{\text{PP}} = -2K \frac{3\Psi_2^{\text{K}}}{2\bar{\varrho}^2}. \quad (44e)$$

Recall that the only non-zero Kinnersley projection is

$$\Psi_2^{\text{K}} = -\frac{M}{\bar{\varrho}^3}. \quad (45)$$

Unlike the Weyl scalars, the spin coefficients do not seem to have a simple representation. Both computing them directly from the PP tetrad or using the knowledge of Lorentz transformations (40)–(42) and the spin coefficients of the Kinnersley tetrad result in lengthy expressions. Let us focus on the horizon initial data instead. Moreover, we employ the choice $K \doteq a^2 \sin^2 \theta$ to simplify them further. We find that the non-vanishing spin coefficients on the horizon are as follows

$$\mu_{\text{PP}} \doteq -\frac{r_{\text{p}} + M}{2\Sigma} - \frac{r_{\text{p}} - r_{\text{m}}}{4\Sigma_0}, \quad (46a)$$

$$\lambda_{\text{PP}} \doteq -\frac{a^2 \sin^2 \theta}{\bar{\varrho}^3} - \frac{(r_{\text{p}} - r_{\text{m}}) a^2 \sin^2 \theta}{8Mr_{\text{p}}\bar{\varrho}^2}, \quad (46b)$$

$$\pi_{\text{PP}} \doteq \frac{ir_{\text{p}} \csc \theta}{\sqrt{2} a \bar{\varrho}}, \quad (46c)$$

$$a_{\text{PP}} \doteq -\frac{i \csc \theta}{\sqrt{2} a}, \quad (46d)$$

$$\alpha_{\text{PP}} \doteq -\frac{\cot \theta}{2\sqrt{2} \bar{\varrho}}, \quad (46e)$$

$$\beta_{\text{PP}} \doteq -\frac{i \csc \theta}{2\sqrt{2} a} - \frac{ir_{\text{p}} \csc \theta}{2\sqrt{2} a \bar{\varrho}}, \quad (46f)$$

$$\varepsilon_{\text{PP}} \doteq \frac{Mr_{\text{p}}(\Sigma - 2r_{\text{p}}\bar{\varrho})}{\bar{\varrho}^3 a^2 \sin^2 \theta}, \quad (46g)$$

$$\kappa_{\text{PP}} \doteq -\frac{i(\varrho + 2r_{\text{m}})}{2\sqrt{2}r_{\text{m}}a\sin^3 \theta}, \quad (46h)$$

$$\rho_{\text{PP}} \doteq \frac{r_{\text{m}} - r_{\text{p}}}{16Mr_{\text{p}}}, \quad (46i)$$

$$\sigma_{\text{PP}} \doteq \frac{\Sigma + 2Mr_{\text{p}}}{2\varrho a^2 \sin^2 \theta} - \frac{\bar{\varrho}(\Sigma + 6Mr_{\text{p}} + r_{\text{m}}^2 \sin^2 \theta)}{16M\varrho a^2 \sin^2 \theta}. \quad (46j)$$

In the next step, we still need to use the Lorentz transformation to obtain the desired vectors. Importantly, unlike in (30), this transformation is coordinate independent due to parallel propagation. Therefore, it is sufficient to find the transformation on the horizon. Conveniently, we are already equipped with the expressions (26). Thus, we can evaluate the vectors ℓ_{PP}^a and m_{PP}^a on the horizon and compare them to determine the constant Lorentz transformation that yields the proper tetrad everywhere.

On the horizon, we set $s \doteq 0$ as usual and find that we need to perform a rotation about n^a with the parameter⁶

$$d = -i \frac{r_{\text{p}} - ia \cos \theta_{\text{p}}}{\sqrt{2K}} \stackrel{K=a^2 \sin^2 \theta_{\text{p}}}{=} -\frac{ir_{\text{p}} + \epsilon_{\theta} \sqrt{a^2 - K}}{\sqrt{2K}}, \quad (47)$$

which yields the correct vector ℓ^a . Generally, we might also need a spin to set the vectors m^a and \bar{m}^a identical to (26), nevertheless, (38) is such that no spin is needed.

The final tetrad is given by

$$\ell^a = \ell_{\text{PP}}^a + \bar{d} m_{\text{PP}}^a + d \bar{m}_{\text{PP}}^a + |d|^2 n^a, \quad (48a)$$

$$m^a = m_{\text{PP}}^a + d n^a. \quad (48b)$$

Fixing the tetrad on the horizon also fixes the gauge freedom, which recovers the limit $a \rightarrow 0$.

We already possess some of the initial data for the isolated horizon, since they are unaffected by the null rotation about n^a : μ , λ , Ψ_4 . To obtain the complete set, we need to supplement the spin coefficients π , a , and ε . The full set is:

$$\mu = \mu_{\text{PP}} \doteq -\frac{r_{\text{p}} + M}{2\Sigma} - \frac{r_{\text{p}} - r_{\text{m}}}{4\Sigma_0}, \quad (49a)$$

$$\lambda = \lambda_{\text{PP}} \doteq -\frac{a^2 \sin^2 \theta}{\bar{\varrho}^3} - \frac{(r_{\text{p}} - r_{\text{m}}) a^2 \sin^2 \theta}{8Mr_{\text{p}}\bar{\varrho}^2}, \quad (49b)$$

$$\pi \doteq \frac{(2ia(r_{\text{p}} + M) + r_{\text{m}}(r_{\text{p}} - r_{\text{m}}) \cos \theta) \sin \theta}{4\sqrt{2}M\bar{\varrho}^2}, \quad (49c)$$

$$a \doteq \frac{ia - r_{\text{p}} \cos \theta}{\sqrt{2}\bar{\varrho}^2 \sin \theta}, \quad (49d)$$

$$\varepsilon \doteq \frac{r_{\text{p}} - r_{\text{m}}}{4\Sigma_0}, \quad (49e)$$

on \mathcal{S}_0 and

$$\Psi_4 = \Psi_4^{\text{PP}} = \frac{3MK}{\bar{\varrho}^5}, \quad (50)$$

on \mathcal{N}_0 . It is clear that μ is real, as it should be for non-twisting congruence, and that ε gives the correct surface gravity, using $\kappa(\ell) = \varepsilon + \bar{\varepsilon}$. Recall that the spin coefficient μ gives the expansion of n^a ($2\text{Re} \mu = \hat{\Theta}_n$), λ gives its shear, and a is the connection of \mathcal{S}_0 . The spin coefficients α and β can be obtained from π and a using

$$\pi = \alpha + \bar{\beta}, \quad a = \alpha - \bar{\beta}, \quad (51)$$

where the first equality is a consequence of the gauge chosen by [5, Eq. (34)] for an isolated horizon, which holds for the tetrad (48), and the second is the definition of a , usually introduced under such a gauge.

Note that due to the properties of the isolated horizon and the formulation of the initial value problem [5], it holds that $\rho \doteq \sigma \doteq \kappa \doteq 0$ and $\tau = \nu = \lambda = 0$. On the horizon, we also have $\Psi_0 \doteq \Psi_1 \doteq 0$.

Moreover, the initial data include the angular components of the vector m^a on the horizon. However, these depend on a spin transformation that we could optionally perform since there is freedom in the choice of the vectors m^a and \bar{m}^a of the Krishnan tetrad. We will show a preferred choice of such a transformation and the resulting components of m^a in Sec. IV A.

In Figs. 2–5, the most important Newman–Penrose scalars are shown. They are plotted in Cartesian coordinates given by

$$x = r \sin \theta, \quad z = r \cos \theta. \quad (52)$$

The area inside the outer horizon is intentionally faded toward the inner horizon for two reasons. First, the focus is on the physically relevant outer region, and the precision towards the inner horizon may deteriorate. Second, the quantities typically grow large in magnitude there, and including them in the contour range would obscure the behavior outside the outer horizon. Nevertheless, the extension inside the outer horizon remains valid, and its qualitative character is visible in the figures.

IV. TETRAD IN THE COORDINATES ADAPTED TO THE ISOLATED HORIZONS

While the tetrad (48) does satisfy all the geometrical properties needed to describe an isolated horizon, it is not yet represented in coordinates adapted to the isolated horizon. Such coordinates were introduced in [5]; we will denote them: $(u, s, \vartheta, \varphi)$.

We have, nevertheless, already met two of them. The radial coordinate s is defined to be the affine parameter that helped us ensure parallel propagation of the tetrad. On the other hand, the polar angle ϑ is defined to be constant along each geodesic but otherwise varies in the manifold, just like the Carter constant K , to which it is connected by Eq. (12), where we identified $\theta_{\text{p}} = \vartheta$. Hence, we have $K = a^2 \sin^2 \vartheta$.

⁶ Notice that $a^2 - K \geq 0$.

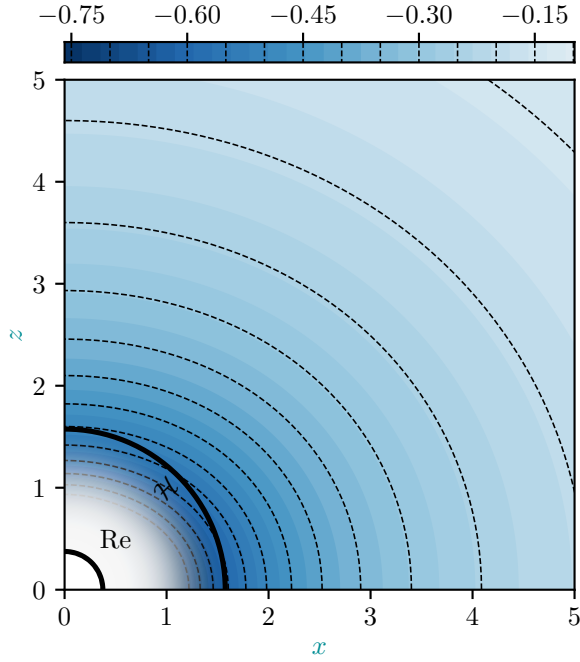


Figure 2. Spin coefficient μ given by tetrad (48) for black hole with $M = 1$ and $a = 0.8$ in the Cartesian version of ingoing null coordinates (52). The imaginary part is zero (as it should be for a non-twisting geodesic congruence) and the displayed real part is the expansion of the congruence (in the direction of n^a).

Let us start by writing differentials for the new coordinates:

$$du = u_{,v} dv + u_{,r} dr + u_{,\theta} d\theta, \quad (53a)$$

$$ds = s_{,r} dr + s_{,\theta} d\theta, \quad (53b)$$

$$d\vartheta = \vartheta_{,r} dr + \vartheta_{,\theta} d\theta, \quad (53c)$$

$$d\tilde{\varphi} = \tilde{\varphi}_{,r} dr + \tilde{\varphi}_{,\theta} d\theta + d\phi, \quad (53d)$$

where we decorated the coordinate φ with a tilde to indicate that it will undergo a slight modification later, yielding the final coordinate u . The coefficients for du are given by $du \equiv n_a dx^a$ so that

$$du = dv - \frac{K}{\mathbb{K}_r + \Sigma_0} dr - \mathbb{K}_\theta d\theta. \quad (54)$$

By construction, see [5], coordinates u , ϑ , and φ are parallel transported off the horizon:

$$n^a \nabla_a u = 0, \quad n^a \nabla_a \vartheta = 0, \quad n^a \nabla_a \varphi = 0, \quad (55)$$

and we require the same also for $\tilde{\varphi}$. While u and ϑ (by means of K) already satisfy this condition, we need to require

$$-\mathbb{K}_r \tilde{\varphi}_{,r} + \mathbb{K}_\theta \tilde{\varphi}_{,\theta} + \frac{aK}{\mathbb{K}_r + \Sigma_0} - a = 0, \quad (56)$$

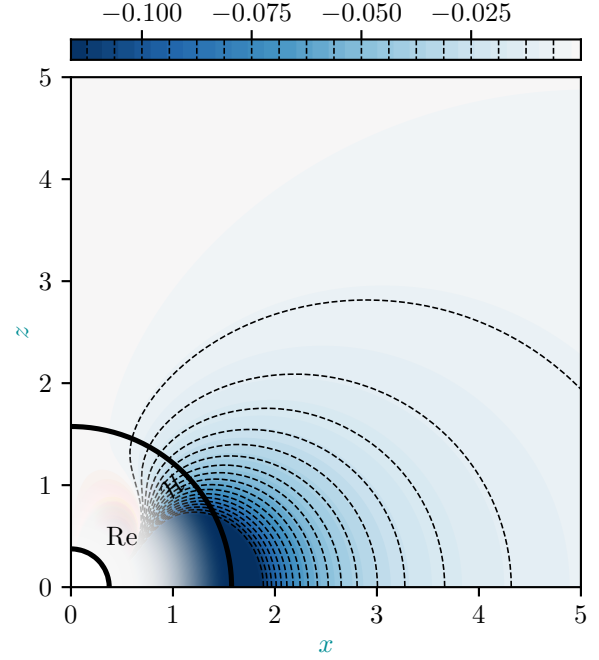


Figure 3. Spin coefficient λ given by tetrad (48) for black hole with $M = 1$ and $a = 0.8$ in the Cartesian version of ingoing null coordinates (52). This spin coefficient represents the shear of the congruence (in the direction of n^a). The plot shows the real part, the imaginary part is zero.

for $\tilde{\varphi}$ to be adapted to isolated horizons. This relation, in turn, fixes the (r, θ) dependence of $\tilde{\varphi}$. Note that the new coordinates are well defined on the horizon.

By inverting relations (53) and transforming the metric (1) into the coordinates $(u, s, \vartheta, \tilde{\varphi})$, we arrive at

$$\begin{aligned} ds^2 = & \left(1 - \frac{2Mr}{\Sigma}\right) du^2 - 2 \left(ds - \frac{s_{,\theta} \Sigma + (\Sigma - 2Mr) \mathbb{K}_\theta + 2Mar \tilde{\varphi}_{,\theta} \sin^2 \theta}{\vartheta_{,\theta} \Sigma} d\vartheta - \frac{2Mar \sin^2 \theta}{\Sigma} d\tilde{\varphi} \right) du \\ & - \frac{\Sigma^2 - (\Sigma - 2Mr) \mathbb{K}_\theta^2 + 4Mar \tilde{\varphi}_{,\theta} \mathbb{K}_\theta \sin^2 \theta + \tilde{\varphi}_{,\theta}^2 (\Sigma \Sigma_0 + 2Ma^2 r \sin^2 \theta) \sin^2 \theta}{\vartheta_{,\theta}^2 \Sigma} d\vartheta^2 \\ & + 2 \sin^2 \theta \frac{\tilde{\varphi}_{,\theta} (\Sigma \Sigma_0 + 2Ma^2 r \sin^2 \theta) + 2Mar \mathbb{K}_\theta}{\vartheta_{,\theta} \Sigma} d\vartheta d\tilde{\varphi} - \frac{(\Sigma \Sigma_0 + 2Ma^2 r \sin^2 \theta) \sin^2 \theta}{\Sigma} d\tilde{\varphi}^2. \end{aligned} \quad (57)$$

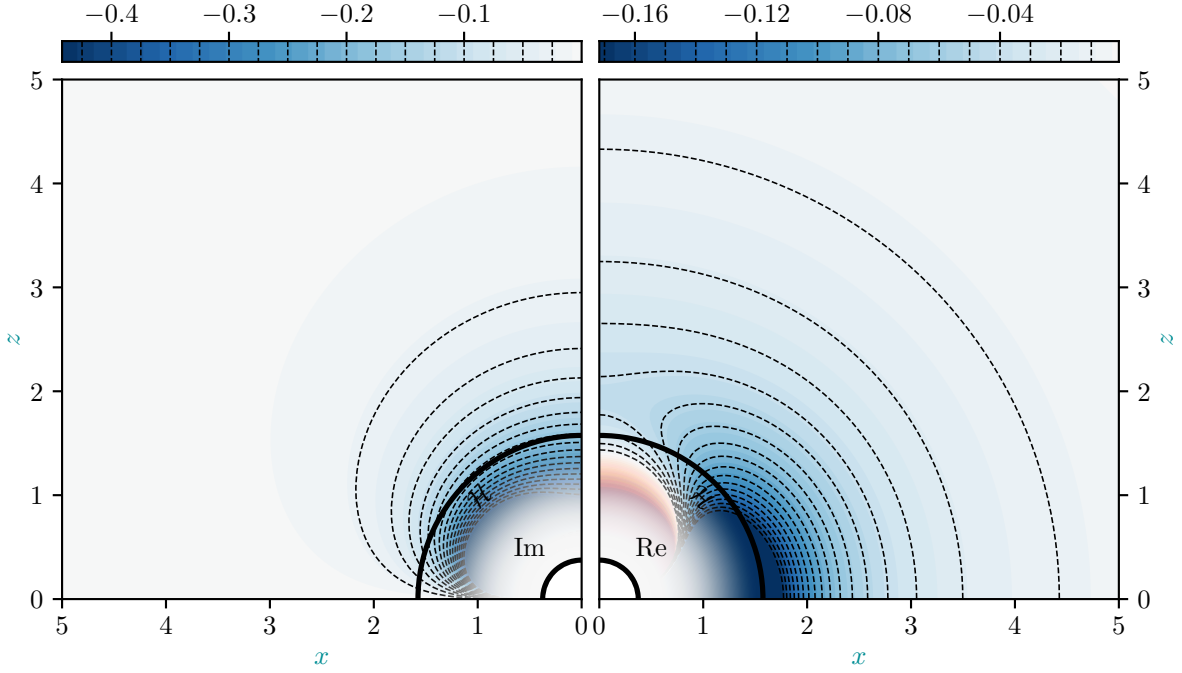


Figure 4. Weyl scalar Ψ_2 given by tetrad (48) for black hole with $M = 1$ and $a = 0.8$ in the Cartesian version of ingoing null coordinates (52). The real (right) and imaginary (left) parts are plotted separately for the same quadrant ($\theta \in (0, \pi/2)$), the imaginary part is mirrored in the plot.

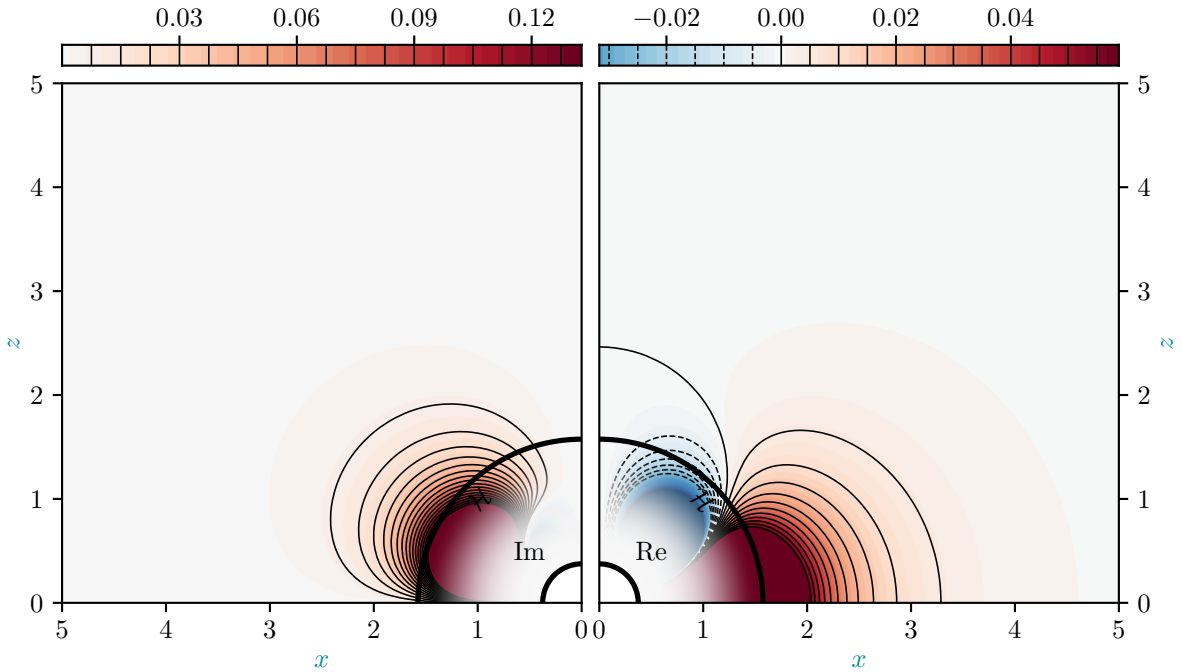


Figure 5. Weyl scalar Ψ_4 given by tetrad (48) for black hole with $M = 1$ and $a = 0.8$ in the Cartesian version of ingoing null coordinates (52). The real (right) and imaginary (left) parts are plotted separately for the same quadrant ($\theta \in (0, \pi/2)$), the imaginary part is mirrored in the plot.

It is worth observing that while the metric is quite complicated, its determinant is very simple:

$$\det g = -\frac{\mathbb{K}_r^2 \sin^2 \theta}{\vartheta, \theta^2}. \quad (58)$$

The parallel-propagated tetrad (38) takes in these coordinates the form

$$\begin{aligned} \ell_{\text{PP}} = \partial_u + \frac{1}{2K \mathbb{K}_r \Sigma} & \left[\left(-\mathbb{K}_r \Sigma (\Sigma + 2\mathbb{K}_\theta s, \theta + s^2) + 2rs \Sigma_0 (\Sigma + \mathbb{K}_\theta s, \theta) + a^2 \mathbb{K}_r s s, \theta \sin(2\theta) \right) \partial_s \right. \\ & - \vartheta, \theta \left(2\mathbb{K}_\theta (\mathbb{K}_r \Sigma - rs \Sigma_0) - a^2 s \mathbb{K}_r \sin(2\theta) \right) \partial_\vartheta \\ & \left. + 2 \left((\mathbb{K}_r \Sigma - rs \Sigma_0) (a - \mathbb{K}_\theta \tilde{\varphi}, \theta) + as (Kr + \mathbb{K}_r \cot \theta (\mathbb{K}_\theta + a \tilde{\varphi}, \theta \sin^2 \theta)) \right) \partial_{\tilde{\varphi}} \right], \end{aligned} \quad (59a)$$

$$n_{\text{PP}} = -\partial_s, \quad (59b)$$

$$\begin{aligned} m_{\text{PP}} = \frac{1}{\sqrt{2K} \mathbb{K}_r \varrho} & \left[\left(a \mathbb{K}_r s, \theta \sin \theta + i (\mathbb{K}_r s \varrho - (\Sigma + \mathbb{K}_\theta s, \theta) \Sigma_0) \right) \partial_s + \vartheta, \theta \left(a \mathbb{K}_r \sin \theta - i \mathbb{K}_\theta \Sigma_0 \right) \partial_\vartheta \right. \\ & \left. + \left(\mathbb{K}_r \csc \theta (\mathbb{K}_\theta + a \tilde{\varphi}, \theta \sin^2 \theta) - i (aK - \Sigma_0 (a - \mathbb{K}_\theta \tilde{\varphi}, \theta)) \right) \partial_{\tilde{\varphi}} \right]. \end{aligned} \quad (59c)$$

In order to obtain the final tetrad, we not only need the constant null rotation about n^a , recall (48). Unfortunately, we also need one additional coordinate transformation – a rigid rotation with the angular velocity of the horizon.⁷ Namely,

$$\varphi = -\frac{a}{r_p^2 + a^2} u + \tilde{\varphi}, \quad (60)$$

where the factor in front of du is chosen so that the ∂_φ component of ℓ^a vanishes on the horizon, recall Eq. (26a). While the transformation itself is trivial, the resulting expressions are substantially lengthier. For that reason, we have chosen not to include it in (53d) and to show the metric and tetrad without it. We leave this trivial addition to the kind reader. It is worth noting that since both u and $\tilde{\varphi}$ are parallel propagated by construction and the factor is constant, φ is also parallel propagated, as it should be.

In the coordinates adapted to the isolated horizon, the tetrad has the special form

$$\ell = \partial_u + U \partial_s + X^2 \partial_\vartheta + X^3 \partial_\varphi, \quad (61a)$$

$$n = -\partial_s, \quad (61b)$$

$$m = \Omega \partial_s + \xi^2 \partial_\vartheta + \xi^3 \partial_\varphi, \quad (61c)$$

and we need to find the metric functions U , X^I , Ω and ξ^I . In Appendix C, relations connecting the (metric functions of) tetrad (59) and tetrad (61) (with the spin applied) can be found. These metric functions depend on the last gauge freedom in the choice of the tetrad that we discuss in the following subsection.

A. Axial isolated horizon

In [11], a preferred choice of tetrad for axially symmetric isolated horizons has been introduced. We now employ this choice to eliminate the remaining freedom in the choice of the angular coordinates and the vectors m^a and \bar{m}^a .

Ashtekar first proposed introducing coordinates ς , φ on \mathcal{S} , the two-sphere foliation of the horizon, such that the two-metric has the form

$$q = -\mathcal{R}^2 (h(\varsigma)^{-1} d\varsigma^2 + h(\varsigma) d\varphi^2), \quad (62)$$

where \mathcal{R} denotes the Euclidean radius defined by the area of the two-sphere \mathcal{S} , which is $A = 4\pi\mathcal{R}^2$. The function $h(\varsigma)$ must satisfy:

$$\begin{aligned} h(\pm 1) &= 0, \\ h'(\pm 1) &= \mp 2, \end{aligned} \quad (63)$$

to avoid conical singularities. Our coordinates are of this form if

$$\tilde{\varphi}, \theta \doteq 0. \quad (64)$$

The Euclidean radius and function h are given as

$$\mathcal{R} = \sqrt{2Mr_p}, \quad h = \frac{2Mr_p \sin^2 \vartheta}{r_p^2 + a^2 \cos^2 \vartheta}. \quad (65)$$

Equipped with such a two-metric, there is a particularly nice choice of the vectors m^a and \bar{m}^a that span the two-

⁷ Note that neither of the two transformations changes the vector n_{PP}^a .

spheres. It is given by:⁸

$$\mathbf{m}_A \doteq -\frac{1}{\sqrt{2}\mathcal{R}} \left(\sqrt{h} \partial_\varsigma - \frac{i}{\sqrt{h}} \partial_\varphi \right). \quad (66)$$

To achieve the canonical form for an axially symmetric isolated horizon, we need to perform an additional *con-**stant* spin transformation, with the coefficient χ_A given by

$$e^{2i\chi_A} = \sqrt{\frac{r_p + ia \cos \vartheta}{r_p - ia \cos \vartheta}}, \quad (67)$$

which does not break the parallel propagation.

V. COORDINATES ADAPTED TO THE ISOLATED HORIZONS

So far, we have constructed a non-twisting parallel-propagated tetrad that is adapted to the isolated horizon. Although we also found the transformation to the coordinates adapted to the isolated horizon, the coordinates have not yet been given explicitly and, consequently, neither has the tetrad. Hence, we need to find the unknown functions s , ϑ (given through K), and φ . They are governed by Eqs. (34), (16), and (56):

$$\mathbb{K}_r s_{,r} - \mathbb{K}_\theta s_{,\theta} = \Sigma, \quad (68)$$

$$\mathbb{K}_r K_{,r} - \mathbb{K}_\theta K_{,\theta} = 0, \quad (69)$$

$$\mathbb{K}_r \tilde{\varphi}_{,r} - \mathbb{K}_\theta \tilde{\varphi}_{,\theta} = \frac{aK}{\mathbb{K}_r + \Sigma_0} - a, \quad (70)$$

with the boundary conditions on the horizon being $s \doteq 0$, $K \doteq a^2 \sin^2 \vartheta$ and $\tilde{\varphi} \doteq \phi$.

Let us start with the simplest case — the axis of rotation where $\theta = 0$. Any choice of K which leads to a finite expansion of n^a on the horizon must satisfy $K(r_p, 0) = 0$. From the rotational symmetry, it follows that

$$K(r, 0) = 0. \quad (71)$$

Using this solution in Eq. (68), we obtain

$$s(r, 0) = r - r_p. \quad (72)$$

Similarly, for $\tilde{\varphi}$, we get from Eq. (56)

$$\tilde{\varphi}(r, 0, \phi) = \phi - \arctan \frac{r}{a} + \arctan \sqrt{\frac{r_p}{r_m}}. \quad (73)$$

On the equator, where $\theta = \frac{\pi}{2}$, the situation is more complicated. By similar arguments, the Carter constant is:

$$K(r, \frac{\pi}{2}) = a^2. \quad (74)$$

⁸ The signs are chosen based on the Kinnersley tetrad, which satisfies such a property in the limit $a \rightarrow 0$.

For s and $\tilde{\varphi}$, we obtain the following equations:

$$s_{,r}(r, \frac{\pi}{2}) = \frac{r^2}{\sqrt{\Sigma_0^2 - a^2 \Delta}}, \quad (75)$$

$$\tilde{\varphi}_{,r}(r, \frac{\pi}{2}) = -\frac{a(r^2 + \sqrt{\Sigma_0^2 - a^2 \Delta})}{\sqrt{\Sigma_0^2 - a^2 \Delta} (\Sigma_0 + \sqrt{\Sigma_0^2 - a^2 \Delta})}. \quad (76)$$

These equations can be solved (integrated) analytically, and they both result in expressions involving elliptical integrals. Nevertheless, the following section presents an approach employing elliptic integrals, with integral of the right side of (75) arising as a special case. For Eq. (76), the corresponding integral is given in the Appendix, Eq (B10).

A. Analytical approach

It might be surprising that it is possible to obtain analytical results. Prescribing the initial data on the horizon, K is being parallel propagated along the geodesics (K varying over the horizon yet constant along a particular geodesic). For null geodesics on the Kerr background, the problem is completely solved. We may either use the approach introduced in [22], which utilizes the Weierstrass \mathcal{p} function and was deployed in [7], or one developed in [10], which takes advantage of elliptic functions.

Since we follow the latter approach, let us first clarify the notation: we use the (incomplete) elliptic integrals of the first kind $F(\phi|m)$ as well as the second kind $E(\phi|m)$. We also use Jacobi elliptic functions, namely $\text{dn}(\phi|m)$, and the Jacobi epsilon function $\mathcal{E}(\phi|m)$. Finally, just like [10], we use exactly the convention of *Wolfram Mathematica*; for exact definitions, see [23].

We are following the notation of [10] and kindly ask the reader to check this reference for all the definitions that we only reference but do not retype in this paper. We initially set $E = 1$, so there is no need to introduce rescaled quantities. The only difference is that [10] uses a different definition of the Carter constant, such that in our notation $K = a^2 + \eta$.

It is convenient to introduce the so-called Mino time τ_M , [10, Eq. (9)],

$$\frac{dx^a}{d\tau_M} = \Sigma n^a, \quad (77)$$

which is measured from the horizon, and converts the four-momentum given by (6) into four decoupled ordinary differential equations. Hence, we first construct

$$r(\tau_M, \vartheta), \quad \theta(\tau_M, \vartheta), \quad (78)$$

and

$$K(r(\tau_M, \vartheta), \theta(\tau_M, \vartheta)) = a^2 \sin^2 \vartheta, \quad (79)$$

and the adapted coordinate ϑ is also the initial angular value on the horizon ($\vartheta \doteq \theta$).

We have the Carter constant $\eta < 0$ and hence we follow the results for Vortical motion in [10, Sec. III.B].

The angular potential $S(\theta)$ has four real roots given by $\cos \theta = \pm \sqrt{u_{\pm}}$, where for our choice of K we have

$$u_+ = 1, \quad u_- = \frac{a^2 - K}{a^2} = \cos^2 \vartheta. \quad (80)$$

Hence, the primitive function [10, Eq. (56)], i.e. $\mathcal{G}_\theta = \int \mathbb{K}_\theta^{-1} d\theta$, can be simplified to

$$\mathcal{G}_\theta = -\frac{\text{sign}(\cos \theta)}{\sqrt{a^2 u_-}} F\left(\arcsin \sqrt{\frac{\cos^2 \theta - u_-}{u_+ - u_-}} \middle| 1 - \frac{u_+}{u_-}\right), \quad (81)$$

then

$$\begin{aligned} \cos \theta_o &= h \sqrt{u_-} \text{dn}\left(\sqrt{a^2 u_-} (\tau_M + \mathcal{G}_\theta^s) \middle| 1 - \frac{u_+}{u_-}\right) \\ &= \cos \vartheta \text{dn}\left(|a \cos \vartheta| (\tau_M + \mathcal{G}_\theta^s) \middle| -\tan^2 \vartheta\right), \end{aligned} \quad (82)$$

where, as defined in [10], the sub/super-scripts o and s stand for observer or source, respectively, and we use the shortcut $h = \text{sign}(\cos \theta)$, also used in [10]. In our case, *the source* is a point on the outer black hole horizon defining the new angular coordinate ϑ (through $\theta \doteq \vartheta$), and *the observer* is anywhere outside (and therefore we will later omit the subscript o).

Later, we will see that the \mathcal{G}_θ for our choice of parameters can be simplified further, but at the moment we need only the fact that it vanishes on the horizon:

$$\mathcal{G}_\theta^s = \mathcal{G}_\theta(\theta = \vartheta) = 0, \quad (83)$$

The structure of the roots of the radial potential R depends on the value of K . For $K \in \langle 0, K_* \rangle$, i.e. from the axis to a certain angular coordinate where $K = K_*$, the roots of the radial potential R consist of two pairs of complex conjugate roots: $r_1, r_2 = \bar{r}_1, r_3, r_4 = \bar{r}_3$. For $K = K_*$, the imaginary parts of r_1, r_2 vanish, i.e. $r_1 = r_2 = r_*$, $r_3 = r_* + ir_i$, $r_4 = \bar{r}_3$, and we have two real roots and a pair of complex conjugate ones $r_1 < r_2, r_3, r_4 = \bar{r}_3$ for $K \in \langle K_*, a^2 \rangle$. The reader is referred to [10, Appendix B, Case (4, 3)] for a detailed discussion and definitions.

To solve for K_* , we need to find the root of the discriminant of R

$$\begin{aligned} 0 &= (M^2 - a^2) K^3 + (a^4 + 30a^2 M^2 - 27M^4) K^2 \\ &\quad - 96a^4 M^2 K + 64a^6 M^2. \end{aligned} \quad (84)$$

This equation has three real roots, and we consider the one for which $K_* \in \langle 0, a^2 \rangle$. Then, we can write down the radial antiderivative $\mathcal{I}_r = \int \mathbb{K}_r^{-1} dr$ given by [10, Eq. (B97), (B101)] and [10, Eq. (B67), (B71)]

$$\mathcal{I}_r = \begin{cases} \frac{2}{C+D} F(\arctan x_4(r) + \arctan g_0 | k_4), & \text{for } K \in \langle 0, K_* \rangle \\ \frac{1}{\sqrt{AB}} F(\arccos x_3(r) | k_3), & \text{for } K \in \langle K_*, a^2 \rangle \end{cases} \quad (85)$$

where the functions A, B, C, D are defined in [10, Eq. (B57)] and [10, Eq. (B85)], and x_3, k_3, x_4, k_4 and g_0 are given by [10, Eqs. (B58), (B59), (B83), (B87), (B88)].

Since we also have the expression for Mino time as

$$\tau_M = \mathcal{I}_r^o - \mathcal{I}_r^s, \quad (86)$$

we can substitute this into Eq. (82) and obtain explicit dependence $\theta = \theta(\vartheta, r)$ as

$$\cos \theta = \cos \vartheta \text{dn}\left(|a \cos \vartheta| (\mathcal{I}_r^o - \mathcal{I}_r^s) \middle| -\tan^2 \vartheta\right). \quad (87)$$

Due to the analytic properties of dn, this relation holds in both hemispheres. While explicitly determining θ , this is still an implicit equation (17) for ϑ . Yet, it is useful when the expansion of $K(r, \theta) = a^2 \sin^2 \vartheta$ is constructed, see Eq. (109), because it allows us to avoid solving the differential equations for the coefficients that arise when (16) is solved using expansions directly.

Since n^r , defined in (6b), is strictly negative along the null congruence under consideration, $r(\mathbf{s})$ is monotone, and we may invert the relation (6b) and write

$$d\mathbf{s} = \frac{\Sigma}{\sqrt{R}} dr. \quad (88)$$

Integrating this, we obtain

$$s = \int \frac{r^2}{\sqrt{R}} dr + \int \frac{a^2 \cos^2 \theta(r)}{\sqrt{R}} dr. \quad (89)$$

The first integral leads to elliptic integrals, see Appendix B (where it is denoted as \mathcal{J}_r), whereas the second one can, taking into account Eq. (87), be easily calculated by a change of variables

$$\frac{1}{\sqrt{R}} dr = d\mathcal{I}_r, \quad (90)$$

and utilizing

$$\int \text{dn}^2(y \mathcal{I}_r | m) d\mathcal{I}_r = \frac{1}{y} \mathcal{E}(y \mathcal{I}_r | m), \quad (91)$$

where y is an arbitrary constant.

This way, we explicitly get $s(r, \vartheta)$ as

$$\begin{aligned} s &= \mathcal{J}(r) - \mathcal{J}(r_p) \\ &\quad + |a \cos \vartheta| \mathcal{E}\left(|a \cos \vartheta| (\mathcal{I}_r(r) - \mathcal{I}_r(r_p)) \middle| -\tan^2 \vartheta\right). \end{aligned} \quad (92)$$

Altogether, (87) and (92) provide an analytic form of the transformations

$$s = s(r, \vartheta), \quad (93)$$

$$\theta = \theta(r, \vartheta). \quad (94)$$

Alas, their inversions seem to be impossible to obtain analytically. The derivation of the first two functions already involves substantial analytical complexity. Extending the same approach to $\tilde{\varphi}$ would still require the inversion of θ and would not yield additional closed-form insight. We therefore defer this function to other approaches that follow.

B. Numerical solution

As we mentioned, Eq. (17) is an implicit equation providing ϑ for given r, θ . Even though both integrals in (17) can be expressed using elliptic integrals, in numerical evaluation, we do this only for \mathcal{G}_θ given by (81). With $u = 1/r$, the radial integral in (17) can be written as

$$\int_{r_p}^r \frac{dr'}{\mathbb{K}_{r'}} = \int_u^{u_p} \frac{du}{\sqrt{(a^2 u^2 + 1)^2 - b^2 u^2 (a^2 u^2 - 2Mu + 1)}}, \quad (95)$$

where $b = a \sin \vartheta$, and then evaluated efficiently using the Gauss–Legendre quadrature. This way, we do not need to evaluate the roots of the radial potential (8) and avoid any problems with reduced precision of elliptic integrals (85) for certain moduli k_3, k_4 . Then, we equate the squares of both integrals appearing in (17). This speeds up the root finding because \mathcal{G}_θ behaves as $\sim |\vartheta - \theta|^{\frac{1}{2}}$.

The coordinate transformations are based on solving ordinary differential equations. Let us discuss here the more complicated situation when the coordinates of (1) are given. Then we first determine ϑ and thus K . Subsequently, we solve the Carter equations rewritten with u as the independent variable. We use quantities $z := (r - r_p) - s$ and $w := |\sin(\vartheta - \theta)|^{1/2}$ to allow $r \rightarrow \infty$ and regularize the differential equation for θ at the horizon. If we now use shortcuts $R(u), \Sigma(u, w), \theta(w)$, the set of differential equations reads

$$\frac{dz}{du} = \frac{\Sigma - \sqrt{R}}{u^2 \sqrt{R}}, \quad (96)$$

$$\frac{dw}{du} = -a \frac{\cos(\vartheta - \theta)}{2u^2 \sqrt{R}} |\sin(\vartheta + \theta)|^{1/2}, \quad (97)$$

$$\frac{d\tilde{\varphi}}{du} = \frac{a}{u^2 \sqrt{R}} \left(1 - \frac{u^2 K}{1 + a^2 u^2 + u^2 \sqrt{R}} \right). \quad (98)$$

Note that $u^2 \sqrt{R}$ as well as $\Sigma - \sqrt{R}$ behave as $\mathcal{O}(1)$ at infinity, i.e. $u \rightarrow 0$. This form of the ordinary differential equation allows for efficient integration because

$$\begin{aligned} \cos^2(\vartheta - \theta) |\sin(\vartheta + \theta)| = \\ (1 - w^4) \left(\sqrt{1 - w^4} |\sin(2\vartheta)| - w^2 \cos(2\vartheta) \right), \end{aligned} \quad (99)$$

and

$$|\cos \theta| = \sqrt{1 - w^4} |\cos \vartheta| + w^2 \sin \vartheta, \quad (100)$$

and therefore the trigonometric functions must be evaluated only at the beginning of the integration. With six steps of ninth-order Runge–Kutta method we get error $\lesssim 10^{-15}$ for $|a| < 0.8, \frac{r_p}{2} < r < \infty$. To reach $|a| \lesssim 1$, we need ten steps or must accept the error $\lesssim 10^{-13}$. This numerical solution is used as a reference to estimate the errors of the series expansions we construct in the subsequent parts of this paper and allows us to plot various

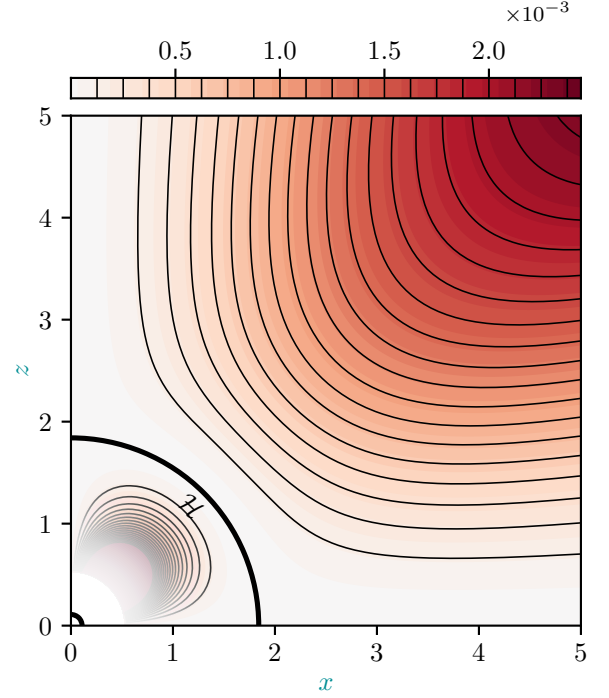


Figure 6. Contour plot adapted from [7, Fig. 3] showing the difference $K - a^2 \sin^2 \theta$ for values $M = 1$ and $a = 1/2$.

quantities for a broader range of parameters than the expansion would allow.

In Fig. 6–8 the functions K, s and $\tilde{\varphi}$ governed by Eqs. (68)–(70) are illustrated using a numerical solution. To better highlight the relevant behavior, the functions are shown through derived expressions.

C. Series expansion around the horizon

While there are obvious advantages to an analytical solution from the previous section, the Jacobi elliptic functions, it is given by, can be unwieldy. For the quasi-local isolated horizon, the close neighborhood of the horizon itself is the section of the space-time that is of the most interest. Therefore, we may construct a series expansion about the horizon of the form

$$K = a^2 \sin^2 \theta + \sum_{j=1}^{\infty} (r - r_p)^j \tilde{C}_j^K(\theta). \quad (101)$$

However, since $K \in \langle 0, a^2 \rangle$, we will instead use a different series expansion, hoping for good convergence at infinity. We may write

$$K = a^2 \sin^2 \theta + \sum_{j=1}^{\infty} \left(1 - \frac{r_p}{r} \right)^j C_j^K(\theta). \quad (102)$$

Solving Eq. (69) order by order, we get (writing C_j^K

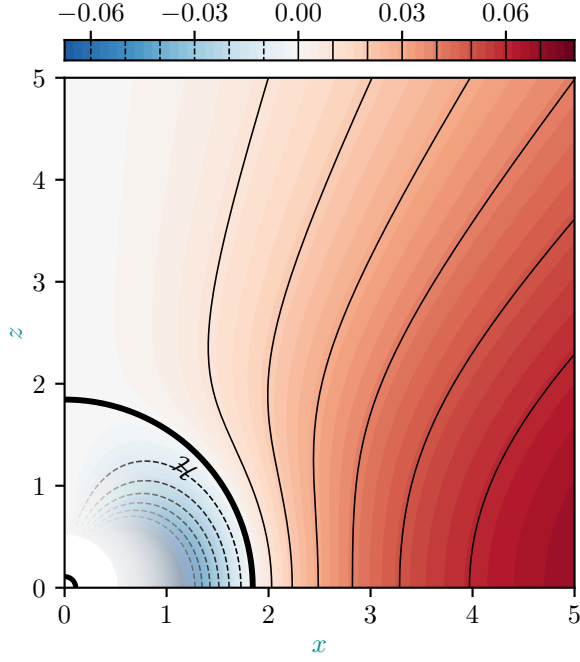


Figure 7. Contour plot demonstrating the difference of the Krishnan and Kerr null coordinates, $(r - r_p) - s$ for values $M = 1$ and $a = 1/2$.

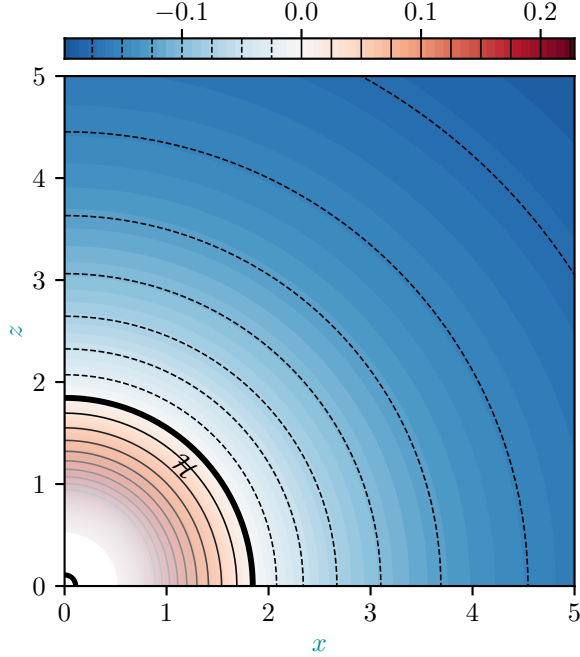


Figure 8. Contour plot demonstrating (r, θ) dependence of the difference $\tilde{\varphi} - \phi$ for values $M = 1$ and $a = 1/2$.

instead of $C_j^K(\theta)$ for simplicity):

$$C_1^K = 0, \quad (103a)$$

$$C_2^K = \frac{a^4 \sin^2(2\theta)}{16M^2}, \quad (103b)$$

$$C_3^K = \frac{a^4 \sin^2(2\theta)}{256M^4} r_m \left(16M + 2(r_m - r_p) \sin^2 \theta \right). \quad (103c)$$

An equation analogous to (69) is valid for ϑ which is connected to K by its choice on the horizon.

As in the case of K , we will seek a solution to Eq. (68) in the form of a series expansion. In this case, in the form

$$s = (r - r_p) + \sum_{j=1}^{\infty} \left(1 - \frac{r_p}{r} \right)^j C_j^s(\theta), \quad (104)$$

where the term $r - r_p$ could, of course, be absorbed into the sum, but we keep it separate to indicate that at infinity $s \sim r$, as expected. The coefficient C_0^s has been set to 0 so that the affine parameter is zero on the horizon.

$$C_1^s = -\frac{a^2 \sin^2 \theta}{2M}, \quad (105a)$$

$$C_2^s = -\frac{a^2 \sin^2 \theta}{32M^3} \left(4a^2 + 5r_m^2 - r_p^2 - r_m(r_m - r_p) \sin^2 \theta \right). \quad (105b)$$

Yet again, we suppose a series expansion (in coordinates r and θ) in the form

$$\tilde{\varphi} = \phi + \sum_{j=0}^{\infty} \left(1 - \frac{r_p}{r} \right)^j C_j^{\tilde{\varphi}}(\theta). \quad (106)$$

and solve Eq. (70). Moreover, by Eq. (64), we have that $C_0^{\tilde{\varphi}} = 0$. The higher order coefficients are

$$C_1^{\tilde{\varphi}} = -\frac{a}{16M^2} \left(3r_m + 4r_p + r_m \cos(2\theta) \right), \quad (107a)$$

$$C_2^{\tilde{\varphi}} = -\frac{a}{2048M^4} r_m \left(89r_m^2 + 247r_p r_m + 176r_p^2 + 12(3r_m^2 + r_p r_m - 4r_p^2) \cos(2\theta) + 3r_m(r_m - r_p) \cos(4\theta) \right). \quad (107b)$$

In the previous section, we showed how to construct a numerical solution. We can use it to deduce the precision we achieve using the series expansion. In Fig. 9, we compare the convergence of the solution through the series expansion (up to the order j) and the numerical solution as given by

$$\Delta_K^j(r, \theta) \equiv -\log_{10} \left| \frac{K_j^{(\text{ser})}(r, \theta) - K^{(\text{num})}(r, \theta)}{K^{(\text{num})}(r, \theta)} \right|. \quad (108)$$

Hence, the value in the plot is the number of digits the series represents correctly. Insight into the convergence behavior of individual terms in the series can be found in Fig. 10.

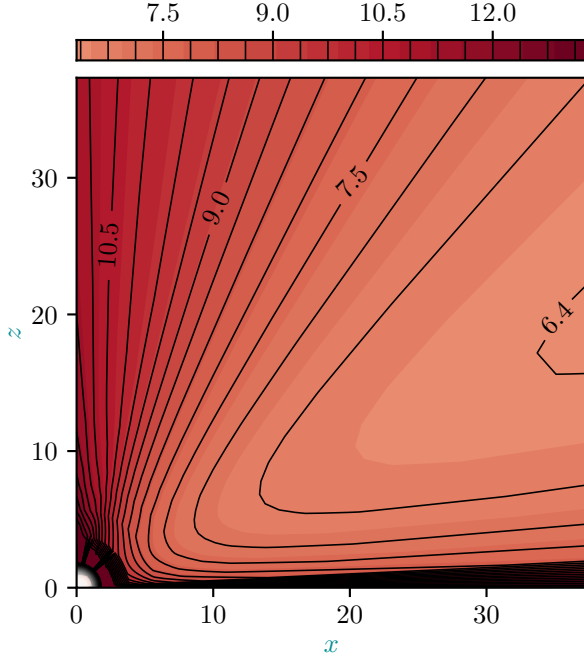


Figure 9. The number of digits correctly represented by the series expansion in the radial direction as estimated by (108). The black hole is taken with mass $M = 1$ and rotational parameter $a = 0.5$. The series expansion used is up to the tenth order.

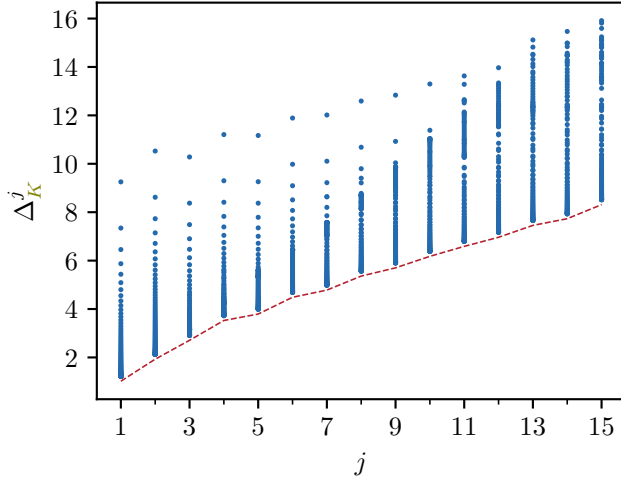


Figure 10. The function Δ_K^j as defined in Eq. (108) for radial series expansion at $20r_p$ with $M = 1$, $a = 1/2$ evaluated for 100 different values (columns of blue dots) of $\theta \in (0, \pi/2)$ (at Chebyshev nodes) for each order j on the horizontal axis. The number on vertical axis corresponds to the number of digits correctly represented by the series expansion and the overall precision is given by the lower edge denoted by red dashed line.

D. Slow rotation series expansion

Let us again start with the Carter constant and a series expansion in the rotational parameter a :

$$K = \sum_{j=0}^{\infty} a^{2j} c_{2j}^K(r, \theta), \quad (109)$$

where we omitted odd powers since K appears as the leading term under a square root, and the zeroth-order term is excluded to enforce reflective symmetry across the equatorial plane, [6].

Solving Eq. (69) we get the first non-zero coefficients (again writing c_j^K instead of $c_j^K(r, \theta)$ for brevity)

$$c_2^K = \sin^2 \theta, \quad (110a)$$

$$c_4^K = \frac{(r - 2M)^2 \sin^2(2\theta)}{16M^2 r^2}, \quad (110b)$$

$$c_6^K = \frac{(r - 2M) \sin^2(2\theta)}{512M^4 r^5} \left(16M^4 + 32M^3 r + 11r^4 - (r - 2M)^2 (4M^2 + 12Mr - 5r^2) \cos(2\theta) \right). \quad (110c)$$

Equation (68) is solved using the series expansion

$$s = \sum_{j=0}^{\infty} a^j c_j^s(r, \theta). \quad (111)$$

The first non-zero coefficients are

$$c_0^s = r - 2M, \quad (112a)$$

$$c_2^s = \frac{5 + 3 \cos(2\theta)}{16M} + \frac{8(r + M) \sin^2 \theta}{16r^2}. \quad (112b)$$

Lastly, the coordinate $\tilde{\varphi}$ is given by Eq. (70). The series expansion

$$\tilde{\varphi} = \sum_{j=0}^{\infty} a^j c_j^{\tilde{\varphi}}(r, \theta), \quad (113)$$

results in non-zero coefficients as

$$c_1^{\tilde{\varphi}} = \frac{1}{r} - \frac{1}{2M}, \quad (114a)$$

$$c_3^{\tilde{\varphi}} = -\frac{29 + 3 \cos(2\theta)}{384M^3} - \frac{3M + 8r - 3 \cos(2\theta)}{24r^4}. \quad (114b)$$

In complete analogy to Figs. 9 and 10, we show the achieved precision of the series in a in Figs. 11 and 12.

In Appendix E, we give the series expansions of the Newman–Penrose spin coefficients and Weyl scalars in the Krishnan coordinates. Moreover, we illustrate both the most important scalars and the effect of black hole rotation on those scalars.

Interestingly, using this approximation, it is actually possible to follow the original approach of [6], now using the revised choice of K (12), and to apply consecutive

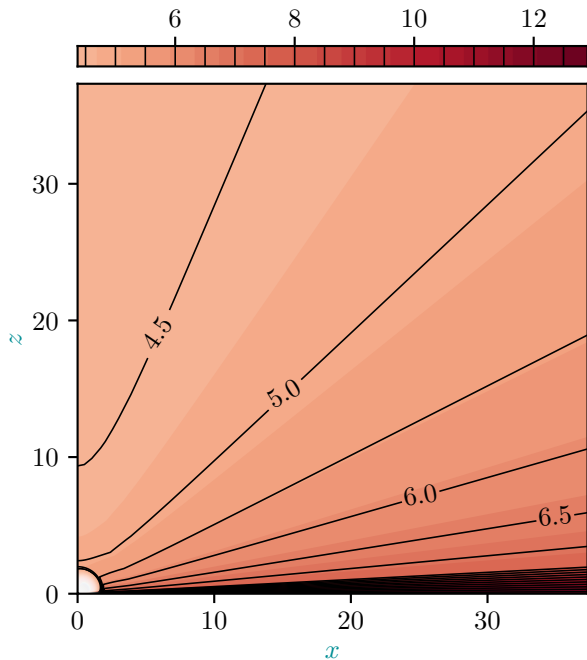


Figure 11. The number of digits correctly represented by the series expansion in the rotational parameter a as estimated by (108). The black hole is taken with mass $M = 1$ and rotational parameter $a = 0.5$. The series expansion used is up to the tenth order.

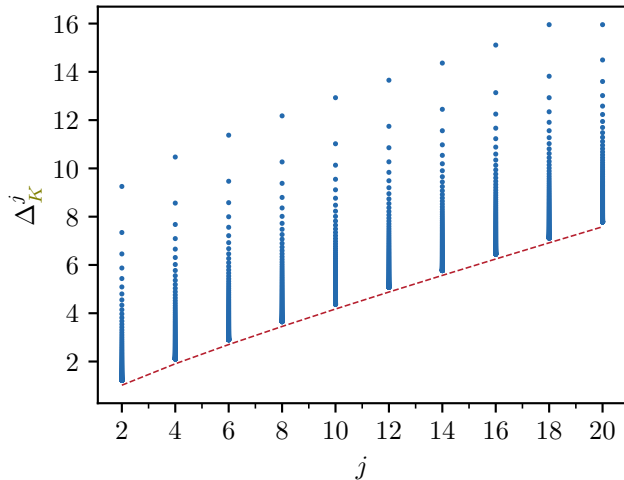


Figure 12. The function Δ_K^j as defined in Eq. (108) for series expansion in a at $20r_p$ with $M = 1$, $a = 1/2$ evaluated for 100 different values (columns of blue dots) of $\theta \in (0, \pi/2)$ (at Chebyshev nodes) for each order j on the horizontal axis. The number on vertical axis corresponds to number of digits correctly represented by the series expansion and the overall precision is given by the lower edge denoted by the red-dashed line.

Lorentz transformations, thereby circumventing the need for the affine parameter s in the search for a geometrically correct tetrad. In fact, this was the approach taken initially, and its results motivated the subsequent investigation. We provide a brief recipe for such an approach in Appendix D.

VI. CONCLUSION

We analyzed the non-twisting geodesic congruence proposed in [7] for describing the isolated horizon of the Kerr black hole, employing the Newman–Penrose tetrad introduced in [5]. The refined congruence is characterized by a Carter constant that remains invariant along each geodesic yet varies across the manifold. By applying the method for constructing parallel-propagated frames from [9], we obtained the complete Newman–Penrose tetrad throughout the entire Kerr space-time.

The resulting tetrad depends on several quantities given by implicit differential equations. These include the Carter constant itself, (minus) the affine parameter of the non-twisting geodesic congruence, and coordinate transformation parameters. Since these objects encode the core computational complexity of the problem, we present multiple strategies for their evaluation, each with distinct benefits and limitations. We provide a fully analytical approach based on an extensive study of null geodesics in Kerr space-time [10], although its reliance on Jacobi elliptic functions often makes it rather unwieldy, and the final coordinate transformations cannot be inverted. As an alternative, we found radial series expansions that yield highly accurate approximations in the immediate vicinity of the horizon, as well as series expansions in the rotational parameter, which remain valid across the entire domain provided the black hole is sufficiently non-extremal. Finally, we tackled the problem through a numerical integration scheme.

Both series-based approaches preserve all isolated-horizon conditions at every order, ensuring that truncated solutions continue to represent legitimate near-equilibrium black holes. These truncated configurations can be viewed as controlled perturbations of the exact Kerr geometry.

Overall, the present work yields an explicit and physically well-adapted construction that improves upon the formulations of [6, 7].

ACKNOWLEDGMENTS

David Kofroň acknowledges support from Grant GACR 23-07457S of the Czech Science Foundation. The authors recognize the use of *xAct* package for *Wolfram Mathematica* [24].

Appendix A: Lorentz transformations in Newman–Penrose formalism

The Newman–Penrose version of the six-parameter Lorentz group is, in the Newman–Penrose formalism, given by two real valued and two complex valued one-parameter subgroups:

- Boosts (with real parameter A):

$$\ell^a \mapsto A^2 \ell^a, \quad n^a \mapsto A^{-2} n^a, \quad m^a \mapsto m^a. \quad (\text{A1})$$

- Spins (with real parameter χ):

$$\ell^a \mapsto \ell^a, \quad n^a \mapsto n^a, \quad m^a \mapsto e^{2i\chi} m^a. \quad (\text{A2})$$

- Null rotations about ℓ^a (with complex parameter c):

$$\begin{aligned} \ell^a &\mapsto \ell^a, \\ n^a &\mapsto n^a + c m^a + \bar{c} \bar{m}^a + |c|^2 \ell^a, \\ m^a &\mapsto m^a + \bar{c} \ell^a. \end{aligned} \quad (\text{A3})$$

- Null rotations about n^a (with complex parameter d):

$$\begin{aligned} \ell^a &\mapsto \ell^a + \bar{d} m^a + d \bar{m}^a + |d|^2 n^a, \\ n^a &\mapsto n^a, \\ m^a &\mapsto m^a + d n^a. \end{aligned} \quad (\text{A4})$$

Appendix B: Integrals

In Sec. IV, we needed to calculate the following integrals

$$\mathcal{I}_r = \int \frac{1}{\sqrt{R}} dr, \quad \mathcal{J}_r = \int \frac{r^2}{\sqrt{R}} dr, \quad (\text{B1})$$

containing the square root of 4th order polynomial

$$R = (r - r_1)(r - r_2)(r - r_3)(r - r_4). \quad (\text{B2})$$

The roots moreover satisfy

$$r_1 + r_2 + r_3 + r_4 = 0, \quad (\text{B3})$$

see [10, Eq. (96)].

For the possible values of the roots we find the following result

$$\mathcal{I}_r = \frac{\mathcal{P}}{\sqrt{R} r_{13} r_{34}} F(\phi_r, m_r), \quad (\text{B4})$$

$$\mathcal{J}_r = \frac{\mathcal{P}}{\sqrt{R}} \left[\frac{r_{42}}{r_{34}} E(\phi_r, m_r) + \frac{r_1 r_{34} + r_3(r_3 + r_4)}{r_{13} r_{34}} F(\phi_r, m_r) \right] + \frac{\sqrt{R}}{r - r_3}, \quad (\text{B5})$$

defining

$$\mathcal{P} = (r - r_3)^2 r_{41} \sqrt{\frac{(r - r_4) r_{13}}{(r - r_3) r_{14}}} \sqrt{\frac{(r - r_1) r_{34}}{(r - r_3) r_{14}}} \sqrt{\frac{(r - r_2) r_{34}}{(r - r_3) r_{24}}}, \quad (\text{B6})$$

where

$$r_{ij} = r_i - r_j, \quad (\text{B7})$$

$$m_r = \frac{r_{32} r_{41}}{r_{31} r_{42}}, \quad (\text{B8})$$

$$\phi_r = \arcsin \sqrt{\frac{(r - r_4) r_{13}}{(r - r_3) r_{14}}}. \quad (\text{B9})$$

It may be tempting to simplify (cancel out some terms) in \mathcal{P} defined in Eq. (B6), but it must be kept in mind that the square roots are complex numbers (the principal branch is considered for our calculations).

Finally, we return to the solution of Eq (76). It is given as

$$\mathcal{I}_{\tilde{\varphi}} = a \frac{\ln\left(1 - \frac{r}{r_p}\right) - \ln\left(1 - \frac{r}{r_m}\right)}{r_m - r_p} + \frac{4aMr(r-r_4)r_2\sqrt{\frac{(r-r_3)r_2}{(r-r_2)r_3}}}{(r_m - r_p)\sqrt{R}r_4\Delta(r_2)\sqrt{\frac{r(r-r_4)r_{42}r_2}{(r-r_2)^2r_4^2}}} \left[(r_p - r_m)F(\phi|m) \right. \\ \left. - (r_p - r_2)\Pi(n(r_m); \phi|m) + (r_m - r_2)\Pi(n(r_p); \phi|m) \right], \quad (\text{B10})$$

where $\Pi(n; \phi|m)$ is the incomplete elliptic integral of the third kind and r_i are the four roots of

$$R = r(r^3 + rr_m r_p + r_m r_p(r_m - r_p)) = 0, \quad (\text{B11})$$

which have the structure

$$r_1 = 0, \quad r_2 = -x - \bar{x}, \quad r_3 = x, \quad r_4 = \bar{x}, \quad (\text{B12})$$

where $\text{Re } x > 0$ and $\text{Im } x > 0$. We also defined the following functions:

$$n(r) = \frac{(r-r_2)r_{41}}{(r-r_1)r_{42}}, \quad (\text{B13})$$

$$\phi = \arcsin \sqrt{\frac{1}{n(r)}}, \quad (\text{B14})$$

$$m = \frac{r_{32}r_{41}}{r_{31}r_{42}}. \quad (\text{B15})$$

This primitive function $\mathcal{I}_{\tilde{\varphi}}$ is a smooth real valued function on $r \in \langle 0, \infty \rangle$ (note, that there is no absolute value in the logarithms; but there are elliptic integrals with complex parameters as well). The manifest logarithmic singularities at r_m, r_p are rectified by the logarithmic singularities of elliptic integrals $\Pi(n(r_m); \phi|m)$, $\Pi(n(r_p); \phi|m)$, which have branch points on the horizons (since for fixed n, m the function $\Pi(n; \phi|m)$ has a branch point for $z = \pm \arcsin(1/\sqrt{n})$). In order to obtain a regular part (and thus the definite integral $\mathcal{I}_{\tilde{\varphi}}(r) - \mathcal{I}_{\tilde{\varphi}}(r_p)$ which enters the coordinate transformation $\phi = \tilde{\varphi} + \mathcal{I}_{\tilde{\varphi}}|_{r_p}$), one has to write the elliptic integrals Π in terms of symmetric Carlson integrals [23] and use the results of [25], in particular [25, Eq. (43)]. Since this computation is demanding (and giving us only $\tilde{\varphi}$ in equatorial plane) and we obtain $\tilde{\varphi}$ by other methods (everywhere), we do not elaborate further.

As well, we understand that we could have used the fact that $r_1 = 0$ in the formulas, but they exhibit some form of symmetry if the r_1 is kept unevaluated.

Appendix C: Tetrad transformations

The final tetrad (61), discussed in Sec. III, obtained from the parallel-propagated tetrad (38) is explicitly given

by the following metric functions:

$$U = U_{\text{PP}} - \frac{r_p^2 + a^2 - K}{2K} - \frac{i r_p - \epsilon_\theta \sqrt{a^2 - K}}{\sqrt{2K}} \Omega_{\text{PP}} \\ + \frac{i r_p + \epsilon_\theta \sqrt{a^2 - K}}{\sqrt{2K}} \bar{\Omega}_{\text{PP}}, \quad (\text{C1a})$$

$$X^2 = X_{\text{PP}}^2 - \frac{i r_p - \epsilon_\theta \sqrt{a^2 - K}}{\sqrt{2K}} \xi_{\text{PP}}^2 \\ + \frac{i r_p + \epsilon_\theta \sqrt{a^2 - K}}{\sqrt{2K}} \bar{\xi}_{\text{PP}}^2, \quad (\text{C1b})$$

$$X^3 = X_{\text{PP}}^3 - \frac{a}{r_p^2 + a^2} - \frac{i r_p - \epsilon_\theta \sqrt{a^2 - K}}{\sqrt{2K}} \xi_{\text{PP}}^3 \\ + \frac{i r_p + \epsilon_\theta \sqrt{a^2 - K}}{\sqrt{2K}} \bar{\xi}_{\text{PP}}^3, \quad (\text{C1c})$$

$$\Omega = \sqrt{\frac{r_p + ia \cos \vartheta}{r_p - ia \cos \vartheta}} \left(\Omega_{\text{PP}} + \frac{i r_p + \epsilon_\theta \sqrt{a^2 - K}}{\sqrt{2K}} \right), \quad (\text{C1d})$$

$$\xi^2 = \sqrt{\frac{r_p + ia \cos \vartheta}{r_p - ia \cos \vartheta}} \xi_{\text{PP}}^2, \quad (\text{C1e})$$

$$\xi^3 = \sqrt{\frac{r_p + ia \cos \vartheta}{r_p - ia \cos \vartheta}} \xi_{\text{PP}}^3. \quad (\text{C1f})$$

Appendix D: Slow rotation expansion approach

In analogy with the approach of [6], we can construct a parallel-propagated tetrad by applying general Lorentz transformations to the Kinnersley tetrad (23). The transformation parameters, taken as a series expansion with coefficients depending on r and θ , are determined by solving the (differential) equations imposed by the conditions of parallel transport.

First, the vector n_K^α is aligned with the chosen geodesic direction, which can be, using the series expansion (109),

written as

$$n_G^\nu = -\frac{\sin^2 \theta}{2r^2} a^2 + \mathcal{O}(a^3), \quad (\text{D1a})$$

$$n_G^r = -1 - \frac{(2M+r)\sin^2 \theta}{2r^3} a^2 + \mathcal{O}(a^3), \quad (\text{D1b})$$

$$n_G^\theta = -\frac{(2M-r)\sin(2\theta)}{4Mr^3} a^2 + \mathcal{O}(a^3), \quad (\text{D1c})$$

$$n_G^\phi = -\frac{1}{r^2} a + \mathcal{O}(a^3). \quad (\text{D1d})$$

To achieve this, both a boost (A1) with parameter A and a null rotation about ℓ^a (A3) parametrized by c are required. These are analogies of (40) and (41).

Next, we need to ensure that the remaining three vectors are parallel propagated. To this end, we can use the remaining two Lorentz transformations — rotation about n^a and spin, neither of which changes the already set vector n^a .

While in Sec. III we first performed the rotation about n^a and then the spin, it is more convenient to switch the order in this case. The parallel propagation is connected to the spin coefficients γ , ν , and τ . Since n^a is parallel propagated, $\nu = 0$. The spin enables us to set $\gamma = 0$ while leaving ν . Note that there is a natural freedom in the choice of the spin parameter, which we can later use to ensure the Ashtekar choice of vectors m^a and \bar{m}^a . While the following rotation about n^a changes γ , the change vanishes for $\nu = 0$, and we can set the parameter such that τ vanishes. However, we also need to inspect the spin coefficients κ , ρ and σ . In the case of these coefficients, we want to ensure they vanish on the horizon. The resulting tetrad is not only parallel propagated, but has the vectors Lie transported on the horizon as it should.

The next step is to find the coordinate transformation to the adapted coordinates. Yet again, we can express the new coordinates as a series expansion with coefficients generally depending on all the old coordinates. We also need a similar series for the old coordinates expressed in terms of the new ones. We can find the coefficients as follows:

- φ based on $n^\varphi = 0$ and $\ell^\varphi \doteq 0$,

- ϑ based on $n^\vartheta = 0$ and $\ell^\vartheta \doteq 0$,
- u based on $n^u = 0$, $m^u = 0$ and $\ell^u \doteq 1$,
- s based on $n^s = -1$ and $\ell^s \doteq 0$.

Additional conditions are needed to fix the freedom in the new coordinates. For the radial coordinate, we want to have $s \doteq 0$. The polar coordinate is best set using relations from Sec. IV A, namely (63).

This leads to an adapted tetrad in adapted coordinates in the form of a series expansion, and it is easy to compute everything else. As a closing note, we found it more convenient to solve the equations for the new radial coordinate such that $\tilde{s} = s + r_p$, and only then correct the expansions by the series of r_p .

Appendix E: Newman–Penrose scalars series expansion in a

With the tetrad constructed, the Newman–Penrose scalars can be easily computed. The most relevant ones are presented in Figs. 13–17. Although the tetrad was primarily displayed up to second order due to its length, it was computed to third order and the same applies to the Newman–Penrose scalars and the figures. The figures are displayed in coordinates \hat{x} and \hat{z} introduced by

$$\hat{x} = (s + r_p) \sin \vartheta, \quad \hat{z} = (s + r_p) \cos \vartheta. \quad (\text{E1})$$

All figures are plotted for $\vartheta \in (0, \pi/2)$ and while the even orders are identical in all quadrants due to symmetries, the odd orders have inverse values for $\hat{z} < 0$.

Each successive order in a is significantly smaller than the preceding one. Instead of plotting the combined amplitude, which would obscure the contributions of higher-order terms, we show each order in a up to a^4 separately. Any order not shown in a given figure corresponds to a vanishing contribution for that scalar.

The expressions for the spin coefficients are:

$$\kappa = -\frac{3is^2 \sin \vartheta}{16\sqrt{2} M (s+2M)^3} a + \frac{s^2 (136M^2 + 80Ms + 11s^2) \sin(2\vartheta)}{128\sqrt{2} M^2 (s+2M)^5} a^2 + \mathcal{O}(a^3), \quad (\text{E2})$$

$$\sigma = \frac{s^2 (40M^2 + 24Ms + 5s^2) \sin(2\vartheta)}{128M^2 (s+2M)^5} a^2 + \mathcal{O}(a^3), \quad (\text{E3})$$

$$\rho = -\frac{s}{2(s+2M)^2} - \frac{3is(4M+s)\cos\vartheta}{8M(s+2M)^3} a + \frac{s^2(6M^2+2Ms+s^2) - 3s(64M^3+46M^2s+10Ms^2+s^3)\cos(2\vartheta)}{64M^2(s+2M)^5} a^2 + \mathcal{O}(a^3), \quad (\text{E4})$$

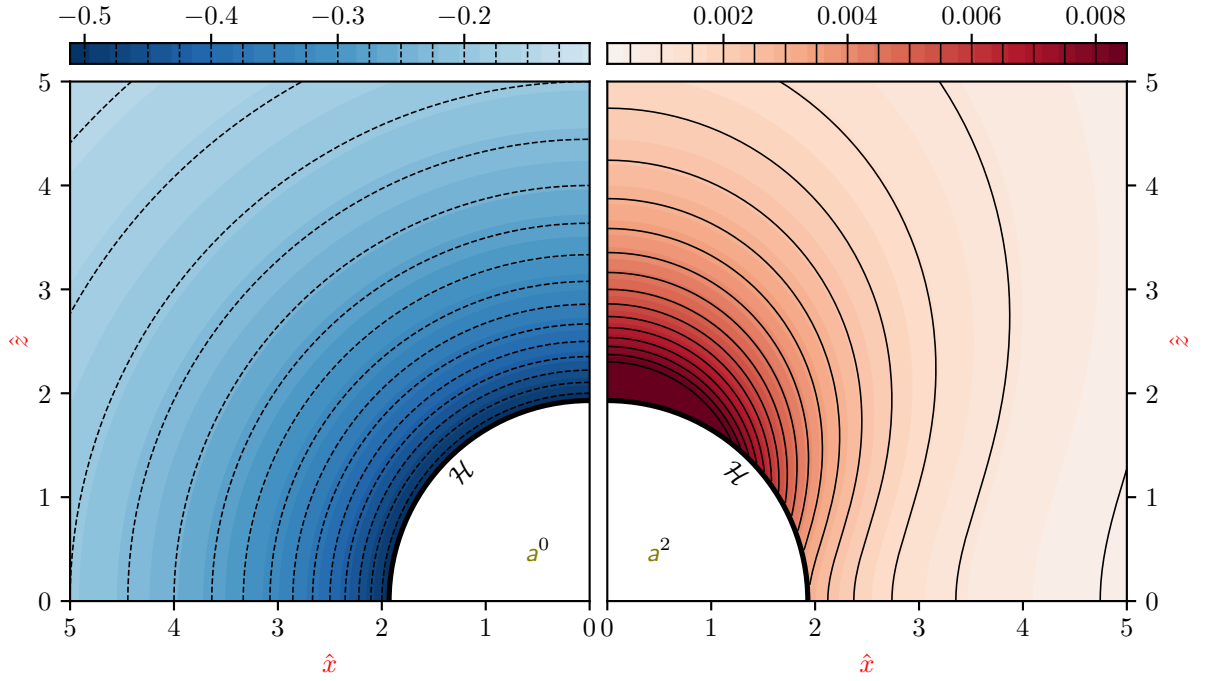


Figure 13. The zeroth and second order terms of the spin coefficient μ . The order is indicated in the area “under the horizon”. The mass of the black hole is set to $M = 1$, and the rotational parameter is $a = 0.3$. Note that both orders are displayed for the same quadrant and are mirrored solely for aesthetic purposes. This spin coefficient is the expansion of the congruence.

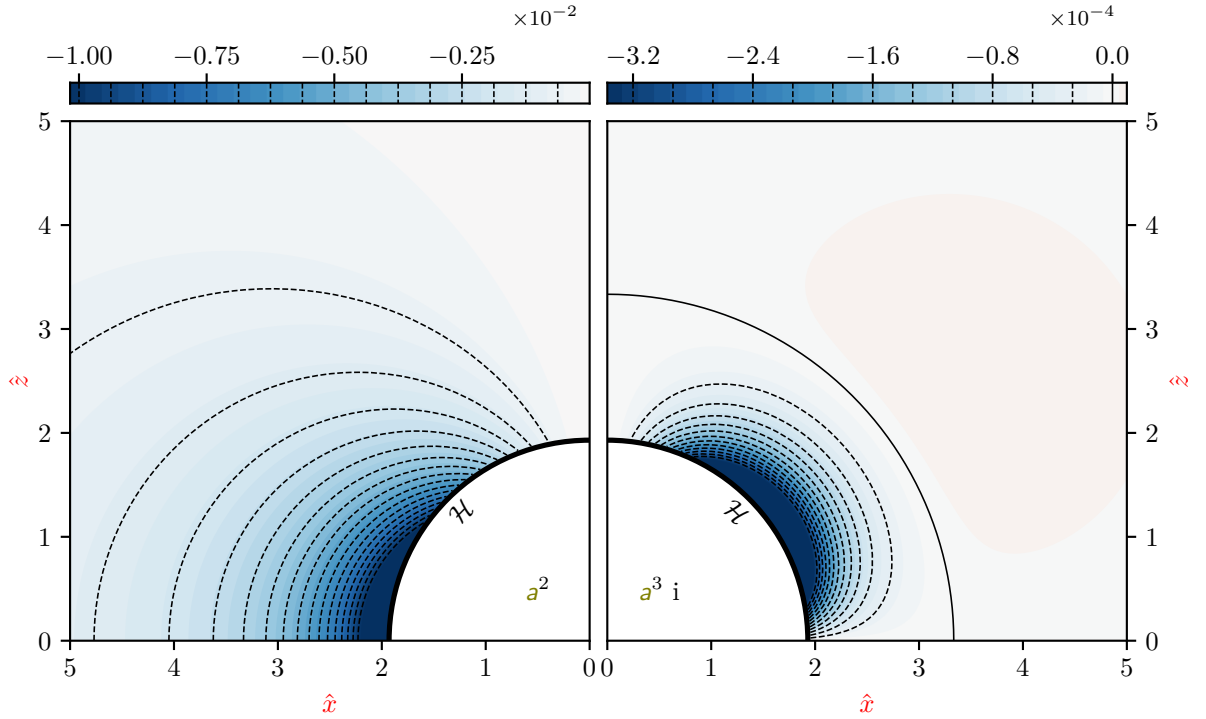


Figure 14. The second and third order terms of the spin coefficient λ . The third order is purely imaginary, which is indicated, together with the order, in the area “under the horizon”. The mass of the black hole is set to $M = 1$, and the rotational parameter is $a = 0.3$. Note that both orders are displayed for the same quadrant and are mirrored solely for aesthetic purposes. This spin coefficient is the shear of the congruence.

$$\beta = \frac{\cot \vartheta}{2\sqrt{2}(s+2M)} - \frac{3i \sin \vartheta}{8\sqrt{2}M(s+2M)} a + \frac{2(s+2M)^3 \cot \vartheta + (8M^3 + 16M^2s + 7Ms^2 + s^3) \sin(2\vartheta)}{32\sqrt{2}M^2(s+2M)^4} a^2 + \mathcal{O}(a^3), \quad (\text{E5})$$

$$\alpha = -\frac{\cot \vartheta}{2\sqrt{2}(s+2M)} + \frac{3iM \sin \vartheta}{2\sqrt{2}(s+2M)^3} a - \frac{2(s+2M)^3 \cot \vartheta + M(40M^2 - 8Ms + s^2) \sin(2\vartheta)}{32\sqrt{2}M^2(s+2M)^4} a^2 + \mathcal{O}(a^3), \quad (\text{E6})$$

$$\begin{aligned} \varepsilon = & \frac{M}{2(s+2M)^2} - \frac{3is(4M+s) \cos \vartheta}{16M(s+2M)^3} a \\ & - \frac{256M^4 + 352M^3s + 208M^2s^2 + 72Ms^3 + 9s^4 - 3s(160M^3 + 112M^2s + 24Ms^2 + 3s^3) \cos(2\vartheta)}{256M^2(s+2M)^5} a^2 + \mathcal{O}(a^3), \end{aligned} \quad (\text{E7})$$

$$\pi = \frac{3i(8M^2 + 4Ms + s^2) \sin \vartheta}{8\sqrt{2}M(s+2M)^3} a - \frac{(32M^3 - 24M^2s - 6Ms^2 - s^3) \sin(2\vartheta)}{32\sqrt{2}M^2(s+2M)^4} a^2 + \mathcal{O}(a^3), \quad (\text{E8})$$

$$\lambda = -\frac{(10M^2 + 4Ms + s^2) \sin^2 \vartheta}{4M(s+2M)^4} a^2 + \mathcal{O}(a^3), \quad (\text{E9})$$

$$\mu = -\frac{1}{(s+2M)} - \frac{3 \sin^2 \vartheta}{8M(s+2M)^2} a^2 + \mathcal{O}(a^3). \quad (\text{E10})$$

The remaining spin coefficients τ , γ and ν vanish.

The projections of the Weyl tensor are:

$$\psi_0 = \frac{3s^2(8M+3s)^2 \sin^2 \vartheta}{64M(s+2M)^7} a^2 + \mathcal{O}(a^3), \quad (\text{E11a})$$

$$\begin{aligned} \psi_1 = & -\frac{3i(8M+3s) \sin \vartheta}{8\sqrt{2}(s+2M)^5} a \\ & + \frac{3s(64M^2 + 28Ms + s^2) \sin(2\vartheta)}{32\sqrt{2}M(s+2M)^6} a^2 \\ & + \mathcal{O}(a^3), \end{aligned} \quad (\text{E11b})$$

$$\begin{aligned} \psi_2 = & -\frac{M}{(s+2M)^3} - \frac{3iM \cos \vartheta}{(s+2M)^4} a \\ & - \frac{3(s^2 - (16M^2 - 3s^2) \cos(2\vartheta))}{8(s+2M)^6} a^2 + \mathcal{O}(a^3), \end{aligned} \quad (\text{E11c})$$

$$\begin{aligned} \psi_3 = & -\frac{3iM \sin \vartheta}{\sqrt{2}(s+2M)^4} a \\ & + \frac{3(6M-s) \sin(2\vartheta)}{4\sqrt{2}(s+2M)^5} a^2 + \mathcal{O}(a^3), \end{aligned} \quad (\text{E11d})$$

$$\psi_4 = \frac{3M \sin^2 \vartheta}{(s+2M)^5} a^2 + \mathcal{O}(a^3). \quad (\text{E11e})$$

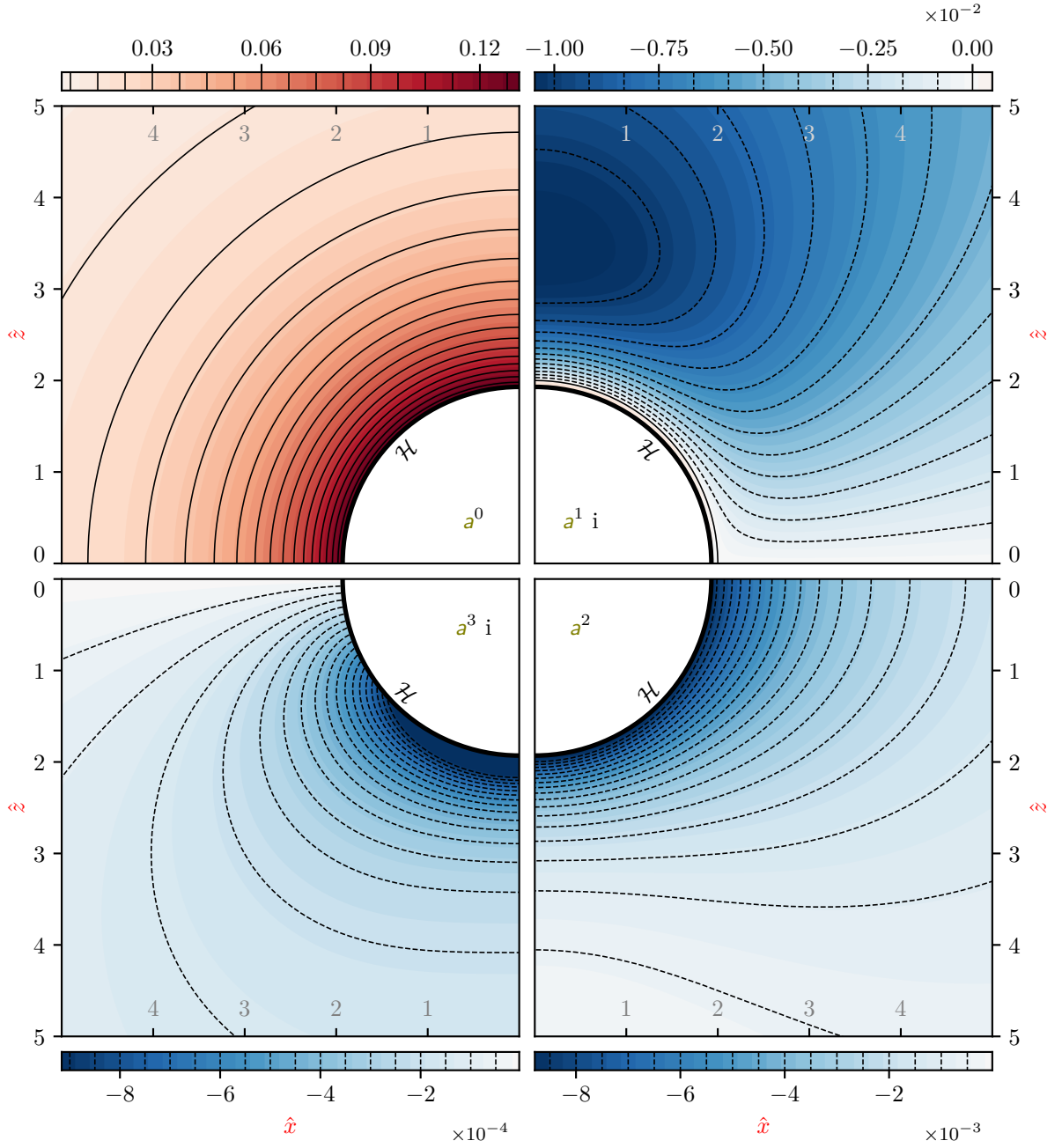


Figure 15. The zeroth (top left) through third (clockwise) order terms of the spin coefficient ϵ . The first and third orders are purely imaginary, which is indicated, together with the order, in the area “under the horizon”. The mass of the black hole is set to $M = 1$, and the rotational parameter is $a = 0.3$. Note that all orders are displayed for the same quadrant and are mirrored solely for aesthetic purposes.

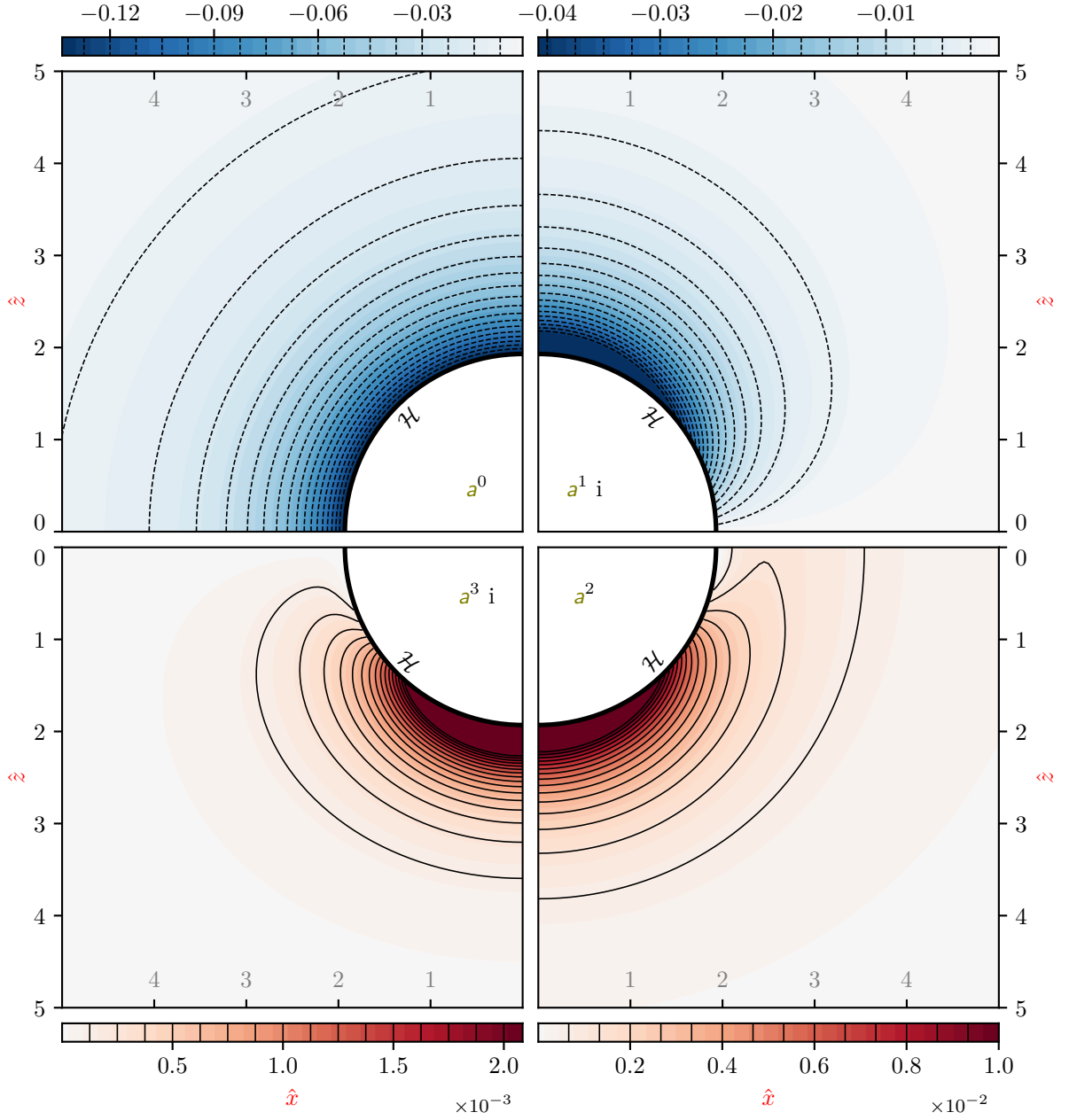


Figure 16. The zeroth (top left) through third (clockwise) order terms of the Weyl scalar Ψ_2 . The first and third orders are purely imaginary, which is indicated, together with the order, in the area “under the horizon”. The mass of the black hole is set to $M = 1$, and the rotational parameter is $a = 0.3$. Note that all orders are displayed for the same quadrant and are mirrored solely for aesthetic purposes.

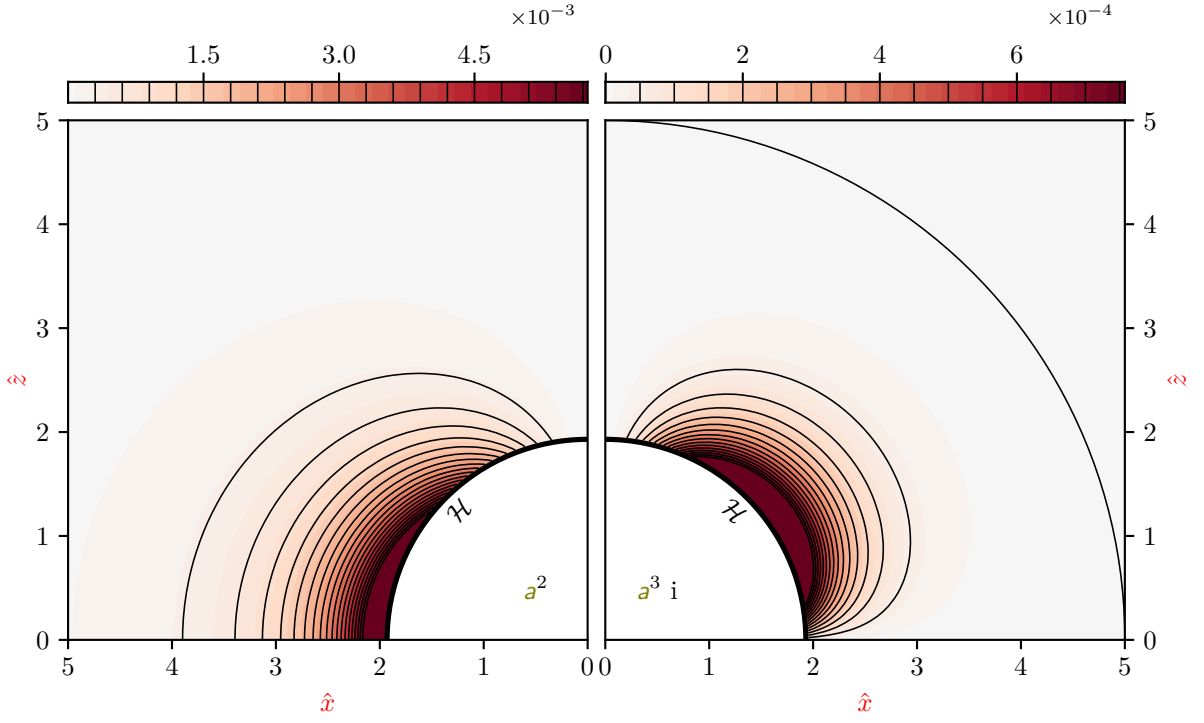


Figure 17. The second and third order terms of the Weyl scalar Ψ_4 . The third order is purely imaginary, which is indicated, together with the order, in the area “under the horizon”. The mass of the black hole is set to $M = 1$, and the rotational parameter is $a = 0.3$. Note that both orders are displayed for the same quadrant and are mirrored solely for aesthetic purposes.

-
- [1] A. Ashtekar, C. Beetle, O. Dreyer, S. Fairhurst, B. Krishnan, J. Lewandowski, and J. Wiśniewski, Generic isolated horizons and their applications, *Physical Review Letters* **85**, 3564 (2000).
- [2] A. Ashtekar, C. Beetle, and J. Lewandowski, Mechanics of rotating isolated horizons, *Physical Review D* **64**, 044016 (2001).
- [3] A. Ashtekar, C. Beetle, and J. Lewandowski, Geometry of generic isolated horizons, *Classical and Quantum Gravity* **19**, 1195 (2002).
- [4] J. Lewandowski, T. Pawłowski, and A. Ashtekar, Geometric characterizations of the Kerr isolated horizon, *International Journal of Modern Physics D* **11**, 739 (2002).
- [5] B. Krishnan, The spacetime in the neighborhood of a general isolated black hole, *Classical and Quantum Gravity* **29**, 205006 (2012).
- [6] M. Scholtz, A. Flandera, and N. Gürlebeck, Kerr-Newman black hole in the formalism of isolated horizons, *Physical Review D* **96**, 064024 (2017).
- [7] D. Kofroň, Kerr black hole in the formalism of isolated horizons, *Physical Review D* **109**, 084029 (2024).
- [8] A. Flandera, D. Kofroň, and T. Ledvinka, Initial data for a deformed isolated horizon, *Physical Review D* **111**, 024020 (2025).
- [9] D. Kubizňák, V. P. Frolov, P. Kratochvíl, and P. Connell, Parallel-propagated frame along null geodesics in higher-dimensional black hole spacetimes, *Physical Review D* **79**, 024018 (2009).
- [10] S. E. Gralla and A. Lupsasca, Null geodesics of the Kerr exterior, *Physical Review D* **101**, 044032 (2020).
- [11] A. Ashtekar, J. Engle, T. Pawłowski, and C. Van Den Broeck, Multipole moments of isolated horizons, *Classical and Quantum Gravity* **21**, 2549 (2004).
- [12] A. Flandera, D. Kofroň, and T. Ledvinka, Kerr isolated horizon revisited: Caustic-free congruence and adapted tetrad, [10.5281/zenodo.17974424](https://arxiv.org/abs/10.5281/zenodo.17974424) (2025).
- [13] E. Poisson, *A Relativist's Toolkit : The Mathematics of Black-Hole Mechanics* (Cambridge University Press, 2004).
- [14] B. Carter, Global structure of the Kerr family of gravitational fields, *Physical Review* **174**, 1559 (1968).
- [15] A. Ashtekar and B. Krishnan, Isolated and dynamical horizons and their applications, *Living Reviews in Relativity* **7**, 10 (2004).
- [16] W. Kinnersley, Type D vacuum metrics, *Journal of Mathematical Physics* **10**, 1195 (1969).
- [17] K. Yano, Some remarks on tensor fields and curvature, *Annals of Mathematics* **55**, 328 (1952).
- [18] E. G. Kalnins, W. Miller, Jr., and G. C. Williams, Killing-Yano tensors and variable separation in Kerr geometry, *Journal of Mathematical Physics* **30**, 2360 (1989).
- [19] J. A. Marck, Solution to the equations of parallel transport in Kerr geometry; Tidal tensor, *Proceedings of the Royal Society of London Series A* **385**, 431 (1983).
- [20] J.-A. Marck, Parallel-tetrad on null geodesics in Kerr-Newman space-time, *Physics Letters A* **97**, 140 (1983).
- [21] N. Kamran and J.-A. Marck, Parallel-propagated frame along the geodesics of the metrics admitting a Killing-Yano tensor, *Journal of Mathematical Physics* **27**, 1589 (1986).
- [22] A. Cieřlik, E. Hackmann, and P. Mach, Kerr geodesics in terms of Weierstrass elliptic functions, *Physical Review D* **108**, 024056 (2023).
- [23] DLMF, *NIST Digital Library of Mathematical Functions*, <https://dlmf.nist.gov/>, Release 1.2.4 of 2025-03-15, F. W. J. Olver, A. B. Olde Daalhuis, D. W. Lozier, B. I. Schneider, R. F. Boisvert, C. W. Clark, B. R. Miller, B. V. Saunders, H. S. Cohl, and M. A. McClain, eds.
- [24] J. M. Martín-García, xAct: Efficient tensor computer algebra for the Wolfram Language, www.xact.es.
- [25] B. C. Carlson and J. L. Gustafson, Asymptotic approximations for symmetric elliptic integrals, *SIAM Journal on Mathematical Analysis* **25**, 288 (1994).